

Density of Spherically-Embedded Stiefel and Grassmann Codes

Renaud-Alexandre Pitaval, Lu Wei, Olav Tirkkonen, and Camilla Hollanti

Abstract

The density of a code is the fraction of the coding space covered by packing balls centered around the codewords. A high density conveys a good performance measure of a code when used as a uniform point-wise discretization of an ambient space. This paper investigates the density of codes in the complex Stiefel and Grassmann manifolds equipped with their commonly used chordal distance, including the unitary group as a special case. The choice of distance enforces the treatment of the manifolds as subspaces of Euclidean hyperspheres. In this geometry, the densest packings are not necessarily equivalent to the maximum-minimum-distance codes. Computing a code's density follows from computing i) the normalized volume of a metric ball and ii) the kissing radius, the radius of the largest balls one can pack around the codewords without overlapping. First, the normalized volume of a metric ball is evaluated by asymptotic approximations. For a small ball, its volume can be well-approximated by the volume of a locally-equivalent tangential ball. In order to properly normalize this approximation, the precise volumes of the manifolds induced by their spherical embedding are computed. For larger balls, a hyperspherical cap approximation is used, which is justified by a volume comparison theorem showing that the normalized volume of a ball in the Stiefel or Grassmann manifold is asymptotically equal to the normalized volume of a ball in its embedding sphere as the dimension grows to infinity. Then, bounds on the kissing radius are derived alongside corresponding bounds on the density. Unlike for spherical codes or for codes in flat spaces, the kissing radius of a Grassmann or Stiefel code cannot be exactly determined from its minimum distance. It is nonetheless possible to derive bounds on density as functions of the minimum distance. Stiefel and Grassmann codes have larger density than their image spherical codes when dimensions tend to infinity. Finally, the bounds on density lead to refinements of the standard Hamming bounds for Stiefel and Grassmann codes.

Renaud-Alexandre Pitaval was Aalto University, Finland, he is now with Huawei Technologies Sweden (email: renaud-alexandre.pitaval@alumni.aalto.fi). Lu Wei is with the School of Engineering and Applied Sciences, Harvard University, USA (email: lwei@g.harvard.edu). Olav Tirkkonen is with the Department of Communications and Networking, Aalto University, Finland (email: olav.tirkkonen@aalto.fi). Camilla Hollanti is with the Department of Mathematics and Systems Analysis, Aalto University, Finland (email: camilla.hollanti@aalto.fi). Part of this work was presented at the 2011 IEEE International Symposium on Information Theory and the 2012 Asilomar Conference of the Signals, Systems and Computers.

I. INTRODUCTION

Sphere packing is a classical problem with a long history from geometry to information theory [1]–[4]. In his 1948 seminal work [5], Shannon made the connection between the capacity of an additive white Gaussian noise channel and packing of multidimensional spheres. This interpretation was later generalized to non-coherent multi-antenna channel as packing in products of Grassmann manifolds [6].

Stiefel and Grassmann codes are matrix codes with applications to Multiple Input Multiple Output (MIMO) communications [6]–[11], Code Division Multiple Access (CDMA) wireless systems [12], and compressive sensing [13], [14]. The complex Stiefel manifold is the space of rectangular semi-unitary matrices. The Grassmann manifold is the space of eigenspaces spanned by the Stiefel matrices. An element in the Grassmann manifold is an equivalence class of Stiefel matrices, which can be alternatively represented by a unique projection matrix. When discussing codes in Grassmann manifolds of one-dimensional subspaces, the equivalent language of frame theory is often used [14].

Depending of the application and convenience, several non-equivalent distances can be defined on these spaces [15], [16]. A common distance for the unitary group and Stiefel manifold is simply the Frobenius norm of the difference of two matrices [17], [18]. Similarly for the Grassman manifold, an often-used distance arises from the Frobenius norm of the difference between two projection matrices [8], [13]. These distances correspond to embedding of the manifolds into an Euclidean space. Through these embeddings, each manifold is a subset of an hypersphere and the distance is the length of a chord.

In the last decade, basic coding-theoretic results estimating the relationship between the cardinality and the minimum distance of codes in Grassmann and Stiefel manifolds have been published [17]–[26]. The standard Hamming bound relates the minimum distance to the notion of code density. The density of a code is the maximum portion of the coding space covered by non-intersecting balls of equal radius. In classical geometry, maximizing the code’s density is known to be equivalent to maximizing its minimum distance. For the Stiefel and Grassmann codes measured by chordal distance, this equivalence does not always hold.

The present paper investigates this surprising fact and discusses the density of codes in Grassmann and Stiefel manifolds equipped with their chordal distance. There are two main difficulties in evaluating the density of codes in these spaces: 1) evaluating the normalized volume of a ball, and 2) estimating the kissing radius of codes.

The problem of estimating the volume of a metric ball has been addressed in [10], [17]–[19], [24]–[27]. In the large code regime, balls are small and can be approximated to be balls in flat space. While

some exact evaluations were obtained in Grassmannian cases [10], [24], the case of the Stiefel manifold has been less addressed. A powerful and general framework is provided in [18], [25], [26]. However, it appears that the state-of-the-art volumes in the literature do not correspond to the desired metrics. Indeed, the volume element is unique up to a non-vanishing scaling factor which is often dismissed, as it can be absorbed in the overall normalization. From Nash embedding theorem [28], every Riemannian metric can be seen as induced by an appropriate Euclidean embedding. There exists an intrinsic metric locally equivalent to the chordal distance, and thus a consistent volume density that defines the notion of volume on the manifold. In this respect, we provide the exact scaling of the volume for Grassmann and Stiefel manifolds induced by the spherical embedding, leading in turn to precise small ball approximations.

For larger radius, we show that the volume of a ball in the manifold can be well approximated by the “area” of the hyperspherical cap the ball is embedded into. The approximation is supported by a volume comparison theorem showing that the normalized volume of a ball in the manifold is asymptotically equal to the normalized volume of a ball in the embedding sphere. This result generalizes and provides a structural unification of our previous results in [29]–[31]. The derivation is a by-product of the asymptotic Gaussianity of the chordal distance arising through its reduction to linear statistics. The intuition behind relates to a classical result by Borel [32] who proved that coordinates of a hypersphere are asymptotically Gaussian as the dimension tends to infinity [33], and the long history of central limit theorems showing the Gaussian behavior of linear statistics [34] in random matrix theory.

Next, the paper addresses the evaluation of the kissing radius and density of Grassmann and Stiefel codes. The kissing radius is the analog of the packing radius for linear codes [35], which has applications in, e.g., sphere-decoder optimization [36], [37]. It is the largest possible radius of packing balls around the codewords of a code. The kissing radius also relates to rate-distortion theory as it is the smallest possible distance from a codeword to the border of its Voronoi cell. The problem reduces to finding the minimum mid-distance between two points at a given distance δ . For a geodesic distance on a flat space, the answer is simply $\delta/2$, the so-called packing radius. With a strictly extrinsic distance, the triangle inequality is never satisfied with equality and the kissing radius is greater than $\delta/2$. While for spherical codes there is a one-to-one mapping between the kissing radius and the minimum distance, this is not the case for the Grassmann and Stiefel codes with chordal distance. As a consequence, the density is not a single-variable function of the minimum distance of the code, and two codes with equal minimum distance could have different densities. This is in sharp contrast with classical packing problems where maximizing the density is equivalent to maximizing the minimum distance. The kissing radius and the density cannot be determined solely from the minimum distance but it is possible to derive bounds.

TABLE I

MANIFOLDS OF DIMENSION \dim WITH THEIR SPHERICAL EMBEDDINGS: $(\mathcal{M}, d_c) \hookrightarrow \mathcal{S}^{D-1}(R)$.

\mathcal{M}	\dim	$d_c(\mathbf{U}, \mathbf{V})$	D	R
\mathcal{U}_n	n^2	$\ \mathbf{U} - \mathbf{V}\ _F$	$2n^2$	\sqrt{n}
$\mathcal{V}_{n,p}^{\mathbb{C}}$	$2np - p^2$	$\ \mathbf{U} - \mathbf{V}\ _F$	$2np$	\sqrt{p}
$\mathcal{G}_{n,p}^{\mathbb{C}}$	$2np - 2p^2$	$\frac{1}{\sqrt{2}}\ \mathbf{U}\mathbf{U}^H - \mathbf{V}\mathbf{V}^H\ _F$	$n^2 - 1$	$\sqrt{\frac{p(n-p)}{2n}}$

Combining these bounds with the volume comparison theorem discussed above shows that the densities of Grassmann and Stiefel codes are asymptotically greater than or equal to the densities of their image spherical codes. The bounds are shown to be tight by simulations.

Finally, a direct application of bounds on density is to revisit the Hamming bounds. The results of this paper improve the Hamming bound for the Grassmann case in [18], [19]; and generalize the bound for the unitary group in [17] to the Stiefel manifold.

The rest of this paper is organized as follows. Section II introduces the considered spaces and their geometry. Section III states the problem and necessary definitions. Section IV addresses the problem of the volume of a ball. In Section V, bounds on kissing radius and density are derived. Section VI provides concluding remarks.

II. THE GRASSMANN AND STIEFEL MANIFOLDS

We consider the following Riemann manifolds equipped with a chordal distance induced by their canonical spherical embedding. Throughout the paper, \mathcal{M} stands for the unitary group \mathcal{U}_n , Stiefel manifold $\mathcal{V}_{n,p}^{\mathbb{C}}$, or Grassmann manifold $\mathcal{G}_{n,p}^{\mathbb{C}}$ embedded into the sphere $\mathcal{S}^{D-1}(R)$ of radius $R = \sqrt{n}$, \sqrt{p} or $\sqrt{\frac{p(n-p)}{2n}}$, in a Euclidean space of dimension $D = 2n^2$, $2np$ or $n^2 - 1$, respectively. Elements in the manifold are represented by matrices in $\mathbb{C}^{n \times n}$ or $\mathbb{C}^{n \times p}$ endowed by the inner product $\langle \cdot, \cdot \rangle = \Re \text{Tr} \cdot^H$, where \Re is the real part and Tr is the matrix trace. The geometric description below follows directly by generalizing [16] and [15] to the complex space. The chordal distances and the corresponding embeddings of these manifolds are summarized in Table I.

A. Hypersphere

The Euclidean $(D - 1)$ -sphere of radius R in \mathbb{R}^D is defined as

$$\mathcal{S}^{D-1}(R) = \{\mathbf{x} \in \mathbb{R}^D \mid \|\mathbf{x}\|_2 = R\}. \quad (1)$$

For $R = 1$, one may simply write \mathcal{S}^{D-1} . The *chordal distance* is the natural Euclidean distance applied to elements on the sphere. Given $\mathbf{x}, \mathbf{y} \in \mathcal{S}^{D-1}(r)$ it is simply the norm of the difference:

$$d_c(\mathbf{x}, \mathbf{y}) = \|\mathbf{x} - \mathbf{y}\|_2. \quad (2)$$

It is an extrinsic distance as it measures the length of a chord outside of the manifold itself, which here is the surface of the sphere.

B. Unitary Group

The *unitary group* is the set of unitary matrices,

$$\mathcal{U}_n = \{ \mathbf{U} \in \mathbb{C}^{n \times n} \mid \mathbf{U}^H \mathbf{U} = \mathbf{U} \mathbf{U}^H = \mathbf{I}_n \}, \quad (3)$$

where \cdot^H denotes the Hermitian conjugate. This compact Lie group is a manifold of dimension $\dim \mathcal{U}_n = n^2$. By differentiating the unitary constraint, one can verify that the tangent space $\mathcal{T}_U \mathcal{U}_n$ at \mathbf{U} is the set of matrices $\mathbf{\Delta} \in \mathbb{C}^{n \times n}$ such that $\mathbf{U}^H \mathbf{\Delta}$ is skew-Hermitian. Specifically, at identity, the tangent space $\mathcal{T}_I \mathcal{U}_n$ is the Lie algebra of skew-Hermitian $n \times n$ matrices $\mathfrak{u}(n)$.

Without loss of generality, one can parametrize the space in terms of skew-Hermitian matrices as $\mathbf{V} = \mathbf{U} \exp(\mathbf{U}^H \mathbf{\Delta}) \in \mathcal{U}_n$ with $\mathbf{U}^H \mathbf{\Delta} \in \mathfrak{u}(n)$. For a fixed $\mathbf{\Delta}$, the exponential map $\exp(\cdot)$ defines the geodesic between \mathbf{U} and \mathbf{V} by mapping the tangent space to the manifold as $\mathbf{V}(t) = \mathbf{U} \exp(t \mathbf{U}^H \mathbf{\Delta})$ with $0 \leq t \leq 1$. A Riemannian metric may be defined from the canonical embedding of \mathcal{U}_n in the Euclidean space $(\mathbb{C}^{n \times n}, \langle \cdot, \cdot \rangle)$, then $\exp(\cdot)$ is the matrix exponential.

Consider the eigenvalue decomposition $\mathbf{U}^H \mathbf{V} = \mathbf{\Omega} \text{diag}(e^{i\theta_1}, e^{i\theta_2}, \dots, e^{i\theta_n}) \mathbf{\Omega}^H$ where the diagonal elements of $\mathbf{\Omega} \in \mathcal{U}_n$ are non-negative and real. One can make this decomposition unique if the angles can be strictly ordered $\pi \geq \theta_n > \dots > \theta_2 > \theta_1 \geq -\pi$. This leads to the corresponding eigenvalue decomposition $\mathbf{U}^H \mathbf{\Delta} = \mathbf{\Omega} \text{diag}(\theta_1, \theta_2, \dots, \theta_n) \mathbf{\Omega}^H$, and accordingly the geodesic between \mathbf{U} and \mathbf{V} becomes

$$\mathbf{V}(t) = \mathbf{U} \mathbf{\Omega} \text{diag}(e^{i\theta_1 t}, e^{i\theta_2 t}, \dots, e^{i\theta_n t}) \mathbf{\Omega}^H. \quad (4)$$

The geodesic distance is the intrinsic distance between two points obtained by integrating the geodesic path along the manifold. It is given by the norm of the tangent direction according to the considered Riemannian metric

$$\begin{aligned} d_g(\mathbf{U}, \mathbf{V}) &= \|\mathbf{\Delta}\|_F = \|\mathbf{U}^H \mathbf{\Delta}\|_F \\ &= \left(\sum_{i=1}^n \theta_i^2 \right)^{1/2}. \end{aligned} \quad (5)$$

Alternatively, the canonical distance in the ambient matrix-space is

$$\begin{aligned}
d_c(\mathbf{U}, \mathbf{V}) &= \|\mathbf{U} - \mathbf{V}\|_F \\
&= \sqrt{2n - 2\Re\text{Tr}(\mathbf{U}^H \mathbf{V})} \\
&= \left(4 \sum_{i=1}^n \sin^2 \frac{\theta_i}{2}\right)^{1/2}
\end{aligned} \tag{6}$$

where the last equality follows from the decomposition (4).

By observing that $d_c(\mathbf{0}, \mathbf{V}) = \|\mathbf{V}\|_F = \sqrt{n}$ for all $\mathbf{V} \in \mathcal{U}_n$, one verifies that the unitary group equipped with d_c has an isometric embedding into the sphere $\mathcal{S}^{2n^2-1}(\sqrt{n})$. The concrete embedding $(\mathcal{U}_n, d_c) \hookrightarrow \mathcal{S}^{2n^2-1}(\sqrt{n})$ is obtained from the classical mapping $\mathbb{C}^{n \times n} \hookrightarrow \mathbb{R}^{2n^2}$ by vectorizing a complex matrix into a real vector.

C. Stiefel Manifold

The complex *Stiefel manifold* is the space of rectangular semi-unitary matrices,

$$\mathcal{V}_{n,p}^{\mathbb{C}} = \{\mathbf{Y} \in \mathbb{C}^{n \times p} \mid \mathbf{Y}^H \mathbf{Y} = \mathbf{I}_p\}. \tag{7}$$

This provides a generalization of both the hypersphere and the unitary group. For $p = n$, one directly recovers $\mathcal{V}_{n,n}^{\mathbb{C}} = \mathcal{U}_n$, while for $p = 1$ and by identification of \mathbb{C}^n with \mathbb{R}^{2n} , this corresponds to the unit sphere $\mathcal{V}_{n,1}^{\mathbb{C}} = \mathcal{S}^{2n-1}$.

As for the unitary group, the tangent space at \mathbf{Y} is the set $\mathcal{T}_{\mathbf{Y}} \mathcal{V}_{n,p}^{\mathbb{C}}$ of matrices $\Delta \in \mathbb{C}^{n \times p}$ such that $\mathbf{Y}^H \Delta \in \mathfrak{u}(p)$ is skew-Hermitian. In general, tangents have the form $\Delta = \mathbf{Y} \mathbf{A} + \mathbf{Y}_{\perp} \mathbf{B}$ where \mathbf{A} is $p \times p$ skew-Hermitian, \mathbf{Y}_{\perp} is the orthogonal complement of \mathbf{Y} such that the concatenation $(\mathbf{Y} \ \mathbf{Y}_{\perp}) \in \mathcal{U}_n$ is unitary, and \mathbf{B} is an $(n-p) \times p$ arbitrary complex matrix. Specifically at “identity” $\mathbf{I}_{n,p} \triangleq \begin{pmatrix} \mathbf{I}_p \\ \mathbf{0} \end{pmatrix}$, tangents are of the form

$$\Delta = \begin{pmatrix} \mathbf{A} \\ \mathbf{B} \end{pmatrix} \in \mathbb{C}^{n \times p} \text{ with } \mathbf{A} \in \mathfrak{u}(p). \tag{8}$$

By counting the degrees of freedom in the tangent space, one finds that the Stiefel manifold is a space with dimension $\dim \mathcal{V}_{n,p}^{\mathbb{C}} = 2np - p^2$.

Given a starting point $\mathbf{Y} = \mathbf{Y}(0)$ and a fixed tangent direction $\Delta = \mathbf{Y} \mathbf{A} + \mathbf{Y}_{\perp} \mathbf{B} \in \mathcal{T}_{\mathbf{Y}} \mathcal{V}_{n,p}^{\mathbb{C}}$, the canonical embedding of $\mathcal{V}_{n,p}^{\mathbb{C}}$ in the Euclidean space $(\mathbb{C}^{n \times p}, \langle \cdot, \cdot \rangle)$ leads to the following geodesic equation [16],

$$\mathbf{Y}(t) = \begin{pmatrix} \mathbf{Y} & \Delta \end{pmatrix} \exp t \begin{pmatrix} \mathbf{Y}^H \Delta & -\Delta^H \Delta \\ \mathbf{I}_p & \mathbf{Y}^H \Delta \end{pmatrix} \mathbf{I}_{2p,p} e^{-t \mathbf{Y}^H \Delta}. \tag{9}$$

The geodesic distance between \mathbf{Y} and $\mathbf{Z} = \mathbf{Y}(1)$ is then

$$d_g(\mathbf{Y}, \mathbf{Z}) = \|\Delta\|_F = (\|\mathbf{A}\|_F^2 + \|\mathbf{B}\|_F^2)^{1/2}. \quad (10)$$

Remark 1. To the best of our knowledge, when $p \neq n$, unlike for the unitary group, it is not known how to compute the geodesic $\mathbf{Y}(t)$ given only $\mathbf{Y} = \mathbf{Y}(0)$ and $\mathbf{Z} = \mathbf{Y}(1)$.

The corresponding Euclidean/chordal distance from the ambient space is

$$d_c(\mathbf{Y}, \mathbf{Z}) = \|\mathbf{Y} - \mathbf{Z}\|_F. \quad (11)$$

Similarly as for the unitary group, one can verify that $d_c(\mathbf{0}, \mathbf{Z}) = \sqrt{p}$ for all \mathbf{Z} , and thus this gives an isometric embedding of the Stiefel manifold $\mathcal{V}_{n,p}^{\mathbb{C}}$ into $\mathcal{S}^{2np-1}(\sqrt{p})$.

As an alternative to (7), the Stiefel manifold can be treated as the quotient space $\mathcal{V}_{n,p}^{\mathbb{C}} \cong \mathcal{U}_n / \mathcal{U}_{n-p}$, where a point in $\mathcal{V}_{n,p}^{\mathbb{C}}$ is an equivalent class of unitary matrices $[\mathbf{U}] = \left\{ \mathbf{U} \begin{pmatrix} \mathbf{I}_p & \mathbf{0} \\ \mathbf{0} & \Omega \end{pmatrix} \mid \Omega \in \mathcal{U}_{n-p} \right\}$. A natural geometry in this interpretation of the Stiefel manifold is the one inherited from the geometry of the unitary group \mathcal{U}_n embedded in $(\mathbb{C}^{n \times n}, \langle \cdot, \cdot \rangle)$. One can split the tangent space of the unitary group at \mathbf{U} between the so-called vertical and horizontal spaces: $\mathcal{T}_{\mathbf{U}}\mathcal{U}_n = \mathcal{H}_{\mathbf{U}} \oplus \mathcal{V}_{\mathbf{U}}$. The vertical space $\mathcal{V}_{\mathbf{U}}$ is the tangent space of $[\mathbf{U}] \hookrightarrow \mathcal{U}_n$ at \mathbf{U} corresponding to “movements” inside the equivalent class. The horizontal space $\mathcal{H}_{\mathbf{U}}$ is the orthogonal complement of the vertical space, providing a unique representation for tangents to the quotient space. For $\mathcal{V}_{n,p}^{\mathbb{C}} \cong \mathcal{U}_n / \mathcal{U}_{n-p}$ at $\mathbf{U} \in \mathcal{U}_n$, it is the collection of matrices $\Delta_* = \mathbf{U} \begin{pmatrix} \mathbf{A} & -\mathbf{B}^H \\ \mathbf{B} & \mathbf{0} \end{pmatrix}$, where $\mathbf{A} \in \mathfrak{u}(n)$ and $\mathbf{B} \in \mathbb{C}^{(n-p) \times p}$. With this non-equivalent geometry, the geodesic distance between \mathbf{U} and $\mathbf{V} = \mathbf{U} \exp(\mathbf{U}^H \Delta_*)$ is $d_{g*}(\mathbf{U}, \mathbf{V}) = \|\Delta_*\|_F = (\|\mathbf{A}\|_F^2 + 2\|\mathbf{B}\|_F^2)^{1/2}$. The metric induced by this embedding, whose resulting volume is discussed in [26], is not considered in this paper.

D. Grassmann Manifold

The complex Grassmann manifold $\mathcal{G}_{n,p}^{\mathbb{C}}$ is the quotient space of $\mathcal{V}_{n,p}^{\mathbb{C}}$ over \mathcal{U}_p :

$$\mathcal{G}_{n,p}^{\mathbb{C}} \cong \mathcal{V}_{n,p}^{\mathbb{C}} / \mathcal{U}_p \subset \mathbb{C}^{n \times p}. \quad (12)$$

Elements in $\mathcal{G}_{n,p}^{\mathbb{C}}$ are equivalent classes of rectangular semi-unitary matrices $\mathbf{Y} \in \mathcal{V}_{n,p}^{\mathbb{C}}$:

$$[\mathbf{Y}] = \{\mathbf{Y}\mathbf{Q} \mid \mathbf{Q} \in \mathcal{U}_p\}. \quad (13)$$

We can identify the equivalent class with a unique matrix representation, which is desirable for practical implementation and computation. As described above, tangent vectors at $\mathbf{Y} \in \mathcal{V}_{n,p}^{\mathbb{C}}$ take the form

$\{\mathbf{Y}\mathbf{A} + \mathbf{Y}_\perp \mathbf{B}\}$. This can be again split between the vertical space $\mathcal{V}_Y = \{\mathbf{Y}\mathbf{A} \mid \mathbf{A} \in \mathfrak{u}_p\}$ and the horizontal space $\mathcal{H}_Y = \{\mathbf{Y}_\perp \mathbf{B} \mid \mathbf{B} \in \mathbb{C}^{n \times (n-p)}\}$. At $\mathbf{I}_{n,p}$, horizontal tangents are thus of the form $\Delta = \begin{pmatrix} \mathbf{0} \\ \mathbf{B} \end{pmatrix}$, and we have $\dim \mathcal{G}_{n,p}^{\mathbb{C}} = 2p(n-p)$. Assume $p \leq n/2$ for simplicity and consider the compact singular value decomposition $\mathbf{B} = \mathbf{L}\mathbf{\Theta}\mathbf{R}^H$, where $\mathbf{L} \in \mathcal{V}_{n-p,p}^{\mathbb{C}}$, $\mathbf{R} \in \mathcal{U}_p$ and $\mathbf{\Theta} = \text{diag}(\theta_1, \dots, \theta_p)$. By setting $\mathbf{A} = \mathbf{0}$, the geodesic equation (9) for the Grassmann manifold reduces to [16]

$$\mathbf{Y}(t) = \mathbf{Y}\mathbf{R}\cos(\mathbf{\Theta}t)\mathbf{R}^H + \mathbf{Y}_\perp \mathbf{L}\sin(\mathbf{\Theta}t)\mathbf{R}^H. \quad (14)$$

The geodesic equation could be rotated from the right by any unitary matrix as it will still belong to the same equivalence class. One can thus restrict without loss of generality the range of the singular values of \mathbf{B} to $0 \leq \theta_i \leq \frac{\pi}{2}$ for all i . These values are known as the principal angles between the planes $[\mathbf{Y}(0)]$ and $[\mathbf{Y}(1)]$. Contrary to Remark 1 for the Stiefel manifold, here given two end points $\mathbf{Y} = \mathbf{Y}(0)$ and \mathbf{Z} , one can compute the tangent in the geodesic (14) and satisfy $[\mathbf{Z}] = [\mathbf{Y}(1)]$ by singular value decomposition of $\mathbf{Z}^H \mathbf{Y}$ and $\mathbf{Z}^H \mathbf{Y}_\perp$, where the singular values of $\mathbf{Z}^H \mathbf{Y}$ are $\cos \theta_1, \dots, \cos \theta_p$.

The geodesic distance is given by

$$\begin{aligned} d_g([\mathbf{Y}], [\mathbf{Z}]) &= \|\Delta\|_F = \|\mathbf{B}\|_F \\ &= \left(\sum_{i=1}^p \theta_i^2 \right)^{1/2}. \end{aligned} \quad (15)$$

In [15], a locally-equivalent distance was defined as

$$d_c([\mathbf{Y}], [\mathbf{Z}]) = \left(\sum_{i=1}^p \sin^2 \theta_i \right)^{1/2}. \quad (16)$$

Rewriting it as

$$\begin{aligned} d_c([\mathbf{Y}], [\mathbf{Z}]) &= \left(p - \sum_{i=1}^p \cos^2 \theta_i \right)^{1/2} = (p - \|\mathbf{Z}^H \mathbf{Y}\|_F^2)^{1/2} \\ &= \frac{1}{\sqrt{2}} \|\mathbf{Y}\mathbf{Y}^H - \mathbf{Z}\mathbf{Z}^H\|_F \end{aligned} \quad (17)$$

reveals that this distance corresponds to a Euclidean embedding, and in fact an isometric embedding into $\mathcal{S}^{n^2-2}(\sqrt{\frac{p(n-p)}{2n}})$ [15]. The embedding follows from mapping any $[\mathbf{Y}] \in \mathcal{G}_{n,p}^{\mathbb{C}}$ to the space of detraced Hermitian matrices as

$$[\mathbf{Y}] \rightarrow \bar{\Pi}_{\mathbf{Y}} = \frac{1}{\sqrt{2}} \left(\mathbf{Y}\mathbf{Y}^H - \frac{p}{n} \mathbf{I} \right), \quad (18)$$

and the chordal distance is the ambient Euclidean distance

$$d_c([\mathbf{Y}], [\mathbf{Z}]) = \|\bar{\Pi}_{\mathbf{Y}} - \bar{\Pi}_{\mathbf{Z}}\|_F^2. \quad (19)$$

In this ambient space of dimension $n^2 - 1$, it can be further verified that the distance of any $\bar{\Pi}_{\mathbf{Y}}$ from the origin is $\|\bar{\Pi}_{\mathbf{Y}} - \mathbf{0}\|_F^2 = \frac{p(n-p)}{2n}$, and thus $\bar{\Pi}_{\mathbf{Y}}$ belongs to a sphere of radius $\sqrt{\frac{p(n-p)}{2n}}$. When there is no ambiguity on the considered space, we will simply write $d_c(\mathbf{Y}, \mathbf{Z})$, which is well-defined as the distance does not depend on the Stiefel representatives.

Alternatively, the Grassmann manifold can be expressed as the quotient space $\mathcal{G}_{n,p}^{\mathbb{C}} \cong \mathcal{U}_n / (\mathcal{U}_p \times \mathcal{U}_{n-p}) \subset \mathbb{C}^{n \times n}$. In this representation, elements in a Grassmann manifold are equivalence classes of unitary matrices. The tangents of $\mathcal{G}_{n,p}^{\mathbb{C}}$ at the identity are of the form $\Delta_* = \begin{pmatrix} 0 & -\mathbf{B}^H \\ \mathbf{B} & 0 \end{pmatrix}$ for this second quotient representation. Again, we do not consider this representation, but we note here that the natural geodesic distance induced by this embedding only differs by a scaling factor

$$\begin{aligned} d_{g*}([\mathbf{Y}], [\mathbf{Z}]) &= \|\Delta_*\|_F = \sqrt{2}\|\mathbf{B}\|_F \\ &= \sqrt{2}d_g([\mathbf{Y}], [\mathbf{Z}]). \end{aligned} \quad (20)$$

III. PACKING PROBLEM AND MAXIMUM CODE DENSITY

A packing is a maximal set of non-intersecting balls of fixed radius, covering enough of the space so that it is not possible to fit in another ball. For a given code size, a packing thus gives the maximum density, i.e. the maximum fraction of the space that one can cover by non-intersecting balls. This problem is considered to be the dual of a coding problem: maximizing the code cardinality for a given minimum distance or reciprocally maximizing the minimum distance for a given code cardinality. Surprisingly, these two problems are not necessarily equivalent for the Grassmann and Stiefel manifolds with chordal distance. This is because there is not necessarily a one-to-one mapping between the minimum distance and the kissing radius of the code, which follows from the choice of an extrinsic distance combined with the *non*-two-point homogeneity of the spaces [22], [38].

A. Code, Minimum Distance, and Metric Balls

An (N, δ) -code is a finite subset of N elements in \mathcal{M} ,

$$\mathcal{C} = \{\mathbf{C}_1, \dots, \mathbf{C}_N\} \subset \mathcal{M}, \quad (21)$$

where δ is the minimum distance defined as

$$\delta = \min\{d_c(\mathbf{C}_i, \mathbf{C}_j) \mid \mathbf{C}_i, \mathbf{C}_j \in \mathcal{C}, i \neq j\}. \quad (22)$$

A metric ball $B_{\mathbf{C}}(\gamma) \subset \mathcal{M}$ of radius γ with center $\mathbf{C} \in \mathcal{C}$ is the subset

$$B_{\mathbf{C}}(\gamma) = \{\mathbf{P} \in \mathcal{M} : d_c(\mathbf{P}, \mathbf{C}) \leq \gamma\} \subseteq \mathcal{M}. \quad (23)$$

B. Kissing Radius

Given a code, one can surround each codeword by metric balls of the same radius and enlarge them until two balls touch. This leads to the notion of *kissing radius*. The kissing radius is a generalization of the so-called *packing radius*. We choose a different terminology to emphasize here that the kissing radius of a code may not be a function of the minimum distance, and also because the packing radius is sometimes defined as $\delta/2$ irrelevantly of the choice of distance [39] by extension from flat geometry.

Definition 1. *The kissing radius of a code \mathcal{C} is the maximum radius of non-overlapping metric balls centered at the codewords:*

$$\varrho_{\mathcal{C}} = \sup_{\substack{B_{C_k}(\gamma) \cap B_{C_l}(\gamma) = \emptyset \\ C_k \neq C_l}} \gamma. \quad (24)$$

For spherical codes there is a one-to-one mapping between the minimum distance and kissing radius. In contrast, for the Grassmann and Stiefel manifolds with chordal distance, the kissing radius and the minimum distance may not be directly expressible as functions of each other. Firstly, the kissing radius corresponds to the mid-distance between two codewords, which may not be the ones at the minimum distance. Secondly, for a given distance, one may have different mid-distances. In general, codes with the same minimum distance may possibly have different kissing radius and different densities.

C. Density

The density of a code is the fraction of \mathcal{M} covered by metric balls centered around the codewords with radius equal to the kissing radius. We consider a uniform measure μ on \mathcal{M} inherited from the Haar measure on the unitary group. Recall that the Grassmann and Stiefel manifolds are homogeneous spaces of the unitary group. For any measurable set $\mathcal{S} \subset \mathcal{M}$ and any $U \in \mathcal{U}_n$, the uniform measure satisfies $\mu(US) = \mu(\mathcal{S})$. Due to the homogeneity of \mathcal{M} , the characteristics of this ball are independent of its center which for convenience will often not be specified. The measure μ corresponds to a normalized volume

$$\mu(B(\gamma)) = \frac{\text{vol } B(\gamma)}{\text{vol } \mathcal{M}}, \quad (25)$$

satisfying $\mu(\mathcal{M}) = 1$.

Definition 2. The density of a code $\mathcal{C} \in \mathcal{M}$ is defined as

$$\begin{aligned}\Delta(\mathcal{C}) &= \mu\left(\bigcup_{\mathcal{C}_i \in \mathcal{C}} B_{\mathcal{C}_i}(\varrho_c)\right) \\ &= \sum_{\mathcal{C}_i \in \mathcal{C}} \mu(B_{\mathcal{C}_i}(\varrho_c)) \\ &= N\mu(B(\varrho_c)).\end{aligned}\tag{26}$$

By definition, it satisfies $\Delta(\mathcal{C}) \leq 1$. A maximum packing code has the maximum density for a given cardinality. In general, the packing problem is not necessarily equivalent to maximizing the minimum distance of the code, as maximizing the kissing radius of the code is not necessarily equivalent to maximizing minimum distance of the code. We illustrate this statement with a concrete example of two analytical codes of cardinality four in the Grassmann manifold $\mathcal{G}_{4,2}^{\mathbb{C}}$ where the (proven) maximum minimum-distance code has a lower density than the other code.

Example 1. Consider the two Grassmannian codes given in Table II. The density of these codes of cardinality four in $\mathcal{G}_{4,2}^{\mathbb{C}}$ is $\Delta = 2\varrho^8$ according to the volume formula provided in [24].

The first code \mathcal{C}_1 is an optimal max-min distance code reaching the spherical simplex bound [15], constructed by embedding the optimal tetrahedron code of $\mathcal{G}_{2,1}^{\mathbb{C}}$ [40]. The embedding is obtained by a tensor product with the identity matrix, a method suggested in [41, Prop. 12]. This is a strongly simplicial configuration in the sense that all principal angles equal $\arccos(\frac{1}{\sqrt{3}})$. The mid-distances between each of the codewords are thus all the same, approximately 0.65, leading to a density of ≈ 0.0638 .

The second code \mathcal{C}_2 is obtained by circular permutation of the rows of the truncated identity matrix. Its distance distribution corresponds to the embedding of a square. The principal angles between two codewords are either $\{0, \frac{\pi}{2}\}$ or $\{\frac{\pi}{2}, \frac{\pi}{2}\}$. The mid-distances between each of the codewords are either $1/\sqrt{2}$ or 1. The density of this code is 0.125, almost twice the density of the optimum max-min distance code \mathcal{C}_1 while it has a smaller minimum distance.

D. Hamming Bound

The notion of density directly relates to the Hamming bound: For any (N, δ) -code, one must satisfy

$$N \leq \frac{1}{\mu(B(\frac{\delta}{2}))}.\tag{27}$$

The upper bound in (27) is a direct application of the standard Hamming bound to \mathcal{M} without taking into account the curvature of the space and the choice of distance. The chordal distance, inherited from

TABLE II

AN EXAMPLE OF A MAXIMAL-MINIMUM-DISTANCE CODE \mathcal{C}_1 WHICH IS NOT AN OPTIMAL PACKING SINCE IT HAS A LOWER DENSITY THAN \mathcal{C}_2 .

\mathcal{C}_1			
density $\Delta = \frac{8}{9} (7 - 4\sqrt{3}) \approx 0.0638$			
min. dist. $\delta = \frac{2}{\sqrt{3}} \approx 1.15$			
kissing radius $\varrho = \sqrt{2}\alpha_- \approx 0.65$			
$\left\{ \begin{bmatrix} \alpha_+ & 0 \\ \alpha_- & 0 \\ 0 & \alpha_+ \\ 0 & \alpha_- \end{bmatrix} \begin{bmatrix} \alpha_+ & 0 \\ -\alpha_- & 0 \\ 0 & \alpha_+ \\ 0 & -\alpha_- \end{bmatrix} \begin{bmatrix} \alpha_- & 0 \\ i\alpha_+ & 0 \\ 0 & \alpha_- \\ 0 & i\alpha_+ \end{bmatrix} \begin{bmatrix} \alpha_- & 0 \\ -i\alpha_+ & 0 \\ 0 & \alpha_- \\ 0 & -i\alpha_+ \end{bmatrix} \right\}$			
where $\alpha_{\pm} = \sqrt{\frac{1}{6}(3 \pm \sqrt{3})}$			

\mathcal{C}_2			
density $\Delta = \frac{1}{8} = 0.125$			
min. dist. $\delta = 1$			
kissing radius $\varrho = \frac{1}{\sqrt{2}} \approx 0.71$			
$\left\{ \begin{bmatrix} 1 & 0 \\ 0 & 1 \\ 0 & 0 \\ 0 & 0 \end{bmatrix} \begin{bmatrix} 0 & 0 \\ 1 & 0 \\ 0 & 1 \\ 0 & 0 \end{bmatrix} \begin{bmatrix} 0 & 0 \\ 0 & 0 \\ 1 & 0 \\ 0 & 1 \end{bmatrix} \begin{bmatrix} 0 & 1 \\ 0 & 0 \\ 0 & 0 \\ 1 & 0 \end{bmatrix} \right\}$			

a Euclidean embedding, is extrinsic to the considered curved space and thus never satisfies the triangle inequality with equality. Accordingly, balls of radius $\delta/2$ around the codewords do not form a packing, as none of the balls would be touching each other and one could possibly fit in an extra ball. Namely, the kissing radius is larger than $\delta/2$, and the Hamming bound can be refined by any radius $\delta/2 < r \leq \varrho$, and ultimately for $r = \varrho$,

$$N \leq \frac{1}{\mu(B(\varrho))}. \quad (28)$$

By construction $\frac{\delta}{2} \leq \varrho$ and thus the Hamming bound (28) is always tighter than the ‘standard Hamming bound’ (27), while being asymptotically equivalent for $\delta \rightarrow 0$.

The difficulty in exploiting the improved bound (28) is to find a relationship between the kissing radius and the minimum distance of the code. To obtain a bound on the minimum distance, one needs to find a function of the minimum distance such that $\delta/2 \leq f(\delta) \leq \varrho$. Then, provided that both the volume expression and f is invertible, it would be possible to bound the minimum distance from above.

IV. VOLUMES

In this section, we address the problem of volume computation in the manifolds, providing two different asymptotic approximations of the volume of balls operating in different regimes.

A. Spherical Volumes and Hyperspherical Caps

The $(D - 1)$ - and D -dimensional volume of $\mathcal{S}^{D-1}(R)$ (with its natural metric d_c) are respectively

$$A_D(R) = \frac{2\pi^{D/2}}{\Gamma(\frac{D}{2})} R^{D-1}, \quad V_D(R) = \frac{\pi^{D/2}}{\Gamma(\frac{D}{2} + 1)} R^D. \quad (29)$$

Since the manifolds of interest are submanifolds of hyperspheres, the considered balls are subsets of hyperspherical caps. A hyperspherical cap is a ball on a sphere,

$$C_{D,R}(r) = \{\mathbf{x} \in \mathcal{S}^{D-1}(R) : \|\mathbf{x} - \mathbf{y}\| \leq r\} \quad (30)$$

for some implicit center \mathbf{y} . One can define a uniform spherical measure σ , and the normalized volume of the spherical caps is denoted by $\sigma(C_{D,R}(r))$. We use a different notation for distinction with the uniform measure on the manifold $\mathcal{M} \subset \mathcal{S}^{D-1}(R)$ but if considering $\mathcal{M} = \mathcal{S}^{D-1}(R)$ then the two measures match $\mu(B(r)) = \sigma(C_{D,R}(r))$.

The volume of a spherical cap can be computed exactly as given below. It is given along with two asymptotics proven in Appendix A.

Lemma 1. *The normalized volume (area) of a hyperspherical cap in $\mathcal{S}^{D-1}(R)$ with chordal distance is given by*

$$\sigma(C_{D,R}(r)) = I_{\frac{r^2}{4R^2}} \left(\frac{D-1}{2}, \frac{D-1}{2} \right) \quad (31)$$

where $I_x(a, b)$ is the regularized incomplete beta function (the radius must satisfy $0 \leq r \leq 2R$).

As the cap's radius r tends to zero, the volume of the spherical cap tends to

$$\lim_{r \rightarrow 0} \sigma(C_{D,R}(r)) = \frac{1}{2\sqrt{\pi}} \frac{\Gamma(\frac{D}{2})}{\Gamma(\frac{D+1}{2})} \left(\frac{r}{R} \right)^{D-1} \quad (32)$$

On the other hand, if the dimension of the sphere D tends to infinity, the volume is

$$\lim_{D \rightarrow \infty} \sigma(C_{D,R}(r)) = \frac{1}{2} \operatorname{erf} \left(\sqrt{\frac{D}{2}} \right) - \frac{1}{2} \operatorname{erf} \left(\sqrt{\frac{D}{2}} \left(1 - \frac{r^2}{2R^2} \right) \right) \quad (33)$$

and $\operatorname{erf}(x)$ is the Gauss error function defined in Eq. (75).

It can be verified that the volume (32) is equal to $V_{D-1}(r)/A_D(R)$. Intuitively, when a cap is small it is almost “flat” and its volume tends to be the “area of a disc”. The volume (33) reveals an asymptotic

Gaussian behavior for large dimensions: the squared chordal distance of uniformly distributed random points is asymptotically Gaussian as $d_c^2 \sim \mathcal{N}\left(2R^2, \frac{4R^4}{D}\right)$ where $\mathcal{N}(m, v)$ is the normal distribution with mean m and variance v . As $D \rightarrow \infty$, high-dimensional random vectors are asymptotically orthogonal and the chordal distance tends to $\sqrt{2}R$ which is the mid-distance between two antipodal points.

B. Manifold Volume and Small Ball Approximation

1) *Overall Manifold Volume:* The volume of a space can be obtained from the integration of a volume element, i.e. an elementary volume unit. The volume element on a Riemannian manifold is unique up to a non-vanishing scaling factor. This scaling factor is induced by the chosen distance, and impacts the overall volume. The theorem below provides the volumes correctly scaled for the chordal distance.

Theorem 1. *The volumes of the manifolds induced by the chordal distance d_c (or its equivalent geodesic distance d_g) are*

- for the unitary group [42]

$$\text{vol } \mathcal{U}_n = \frac{(2\pi)^{\frac{n(n+1)}{2}}}{\prod_{i=1}^n \Gamma(i)}, \quad (34)$$

- for the Stiefel manifold

$$\text{vol } \mathcal{V}_{n,p}^{\mathbb{C}} = \frac{2^{\frac{p(p+1)}{2}} \pi^{np}}{\tilde{\Gamma}_p(n)}, \quad (35)$$

- for the Grassmann manifold

$$\text{vol } \mathcal{G}_{n,p}^{\mathbb{C}} = \pi^{p(n-p)} \prod_{i=1}^p \frac{\Gamma(p-i+1)}{\Gamma(n-i+1)} \quad (36)$$

where the complex multivariate gamma function is

$$\tilde{\Gamma}_p(n) = \pi^{\frac{p(p-1)}{2}} \prod_{i=1}^p \Gamma(n-i+1). \quad (37)$$

A detailed volume computation is provided in Appendix B. While it is possible to find the exact volume for the unitary group rigorously derived for the chordal distance in [42], [43], the equivalent result for the Stiefel manifold does not seem to have been reported before. This volume differs by a constant factor from the commonly cited formula, see e.g. [6], [18], [19]. In many contexts, the overall scaling of the volume is meaningless as often the induced scaling would be absorbed or canceled out. The volumes known in the literature arise from integration of a volume element neglecting scalar prefactors. Conventional volumes in the literature are expressed as the product of the volumes of spheres:

$$\text{vol } \mathcal{V}_{n,p}^{\mathbb{C}} = \prod_{k=n-p+1}^n V_{2k}(1) = \prod_{k=n-p+1}^n \frac{2\pi^k}{\Gamma(k)}, \text{ where } V_{2k}(1) = \text{vol } \mathcal{S}^{2k-1} \text{ is given in (29). The two}$$

different conventions are related by $\text{vol } \mathcal{V}_{n,p}^{\mathbb{C}} = 2^{\frac{p(p-1)}{2}} \text{vol } \mathcal{V}_{n,p}^{\mathbb{C}}$. For the Grassmann manifold with the geometry induced by the spherical embedding, it appears that these normalizations cancel out so that we have $\text{vol } \mathcal{G}_{n,p}^{\mathbb{C}} = \frac{\text{vol } \mathcal{V}_{n,p}^{\mathbb{C}}}{\text{vol } \mathcal{U}_p} = \frac{\text{vol } \mathcal{V}_{n,p}^{\mathbb{C}}}{\text{vol } \mathcal{U}_p} = \frac{\text{vol } \mathcal{U}_n}{\text{vol } \mathcal{U}_p \text{vol } \mathcal{U}_{n-p}}$. However, we remark that the true volume of the Grassmannian with the quotient geometry $\mathcal{G}_{n,p}^{\mathbb{C}} \cong \mathcal{U}_n / (\mathcal{U}_p \times \mathcal{U}_{n-p})$ and distance d_{g*} is $\text{vol}_* \mathcal{G}_{n,p}^{\mathbb{C}} = \frac{\text{vol } \mathcal{U}_n}{\text{vol } \mathcal{U}_p \text{vol } \mathcal{U}_{n-p}}$, which differs from $\text{vol } \mathcal{G}_{n,p}^{\mathbb{C}}$ in the embedding geometry, computed above. Using the conventional volumes, one would get $\text{vol}_* \mathcal{G}_{n,p}^{\mathbb{C}} = \frac{\text{vol } \mathcal{U}_n}{\text{vol } \mathcal{U}_p \text{vol } \mathcal{U}_{n-p}} = \text{vol } \mathcal{G}_{n,p}^{\mathbb{C}}$, i.e. the volumes in the two geometries are erroneously assumed to be the same. When interpreting the Haar measure as a normalized volume (25), keeping track of the scaling of the volume is necessary. We suspect that omitting the volume scaling factors is one of the reasons behind the numerical errors observed in [18], in which a standard volume formula was used irrespectively of the geometric interpretation of the Stiefel and Grassmann manifolds, and the related distances.

Considering d_c , some special manifolds of interest are isometrically isomorphic to spheres: the Stiefel manifolds $\mathcal{V}_{n,1}^{\mathbb{C}} \cong \mathcal{S}^{2n-1}$, and the Grassmann manifolds $\mathcal{G}_{2,1}^{\mathbb{C}} \cong \mathcal{S}^2(\frac{1}{2})$. As expected, the volumes in Theorem 1 match the spherical volume (29) in these cases.

2) *Small Ball Approximation*: The volume of a small *geodesic* ball can be well approximated by the volume of a ball of equal radius in the tangent space. This approximation, tight as the radius goes to zero, is actually an upper bound as discussed in [18], known as the Bishop–Gromov inequality, a volume comparison theorem valid for any Riemannian manifold. In [18], it was used to evaluate volumes of small geodesic balls in the Grassmann and Stiefel manifolds. For the case of the Stiefel manifolds, results were extended to the chordal distance in an indirect manner from the geodesic distance d_{g*} combined with local inequalities. Surprisingly, the results of [24] show that this approximation is exact for the Grassmann manifold *with chordal distance* smaller than one, in the same manner as the area of a cap of the real sphere equals to the area πr^2 of a disk. Later, the same approximation was used in [44] for volumes in simple flag manifolds. Refining the result, a power series expansion for the volume of small geodesic ball in any Riemannian manifold [45] was later leveraged in [25], [26]. Limiting this expansion to the leading term gives

$$\text{vol } B(r) = V_{\dim}(r)(1 + O(r^2)). \quad (38)$$

where $V_{\dim}(r)$ is given according to (29) and the dimension \dim of the manifold in Table I. Intuitively, in a small neighborhood the manifold looks like a Euclidean space and can be approximated by its tangent space. Other coefficients of the series expansion are addressed in [26] requiring computation of the curvature of the manifold.

The expansion (38) given for the geodesic distance extends to the corresponding chordal distance induced by the isometric embedding in \mathbb{R}^D as $d_g = d_c + O(d_c^3)$ [46], [47]. Therefore, the normalized volume of metric balls in \mathcal{M} with dimension \dim for *both* the geodesic distance d_g and the chordal distance d_c is given by

$$\mu(B(r)) = \frac{V_{\dim}(r)}{\text{vol } \mathcal{M}}(1 + O(r^2)) \quad (39)$$

as $r \rightarrow 0$. We then have the following results as a direct consequence of Theorem 1 and $V_D(r)$ given in (29).

Corollary 1. *The volume of metric balls as $r \rightarrow 0$ with metrics d_c or d_g is*

$$\mu(B(r)) = c_{n,p} r^{\dim}(1 + O(r^2)), \quad (40)$$

- where for the Stiefel manifold $\mathcal{V}_{n,p}^{\mathbb{C}}$,

$$c_{n,p} = \frac{2^{-\frac{p(p+1)}{2}} \pi^{\frac{-p}{2}}}{\Gamma(p(n-p/2)+1)} \prod_{i=1}^p \Gamma(n-i+1), \quad (41)$$

- and for the Grassmann manifold $\mathcal{G}_{n,p}^{\mathbb{C}}$ [24],

$$c_{n,p} = \frac{1}{\Gamma(p(n-p)+1)} \prod_{i=1}^p \frac{\Gamma(n-i+1)}{\Gamma(p-i+1)}. \quad (42)$$

For the general case $n \neq p$, the result above is different than the one in [26] derived for quotient geometry (d_{g*}); the two results match for $n = p$ as expected. Comparing to the Grassmannian case in [26], there is a difference by a factor of $2^{2p - \frac{n-p}{2}(n-p+1)}$. The local equivalence between the chordal distance d_c and the geodesic distance d_g makes the result identical for both metrics. For the chordal distance, the result of [24] is stronger as it gives a strict equality for $r < 1$.

The approximated volumes in Corollary 1 for the Stiefel manifold (with $p \neq n$) and for the unitary group (with $p = n$) are compared with simulation in Fig. 1. The figures are shown in logarithm scales since the region of interest is small chordal distance. We see that the approximations match almost exactly the simulations as $r \rightarrow 0$, which is a consequence of the exact volume normalization given in Theorem 1.

C. Complementary Balls

As an interlude, we discuss complementary balls for which small ball approximations could be used to compute the volume of very large balls almost totally covering the space. In the same manner as a sphere can be fully covered by two complementary caps satisfying

$$\sigma(C_{D,R}(r)) = 1 - \sigma(C_{D,R}(\sqrt{4R^2 - r^2})), \quad (43)$$

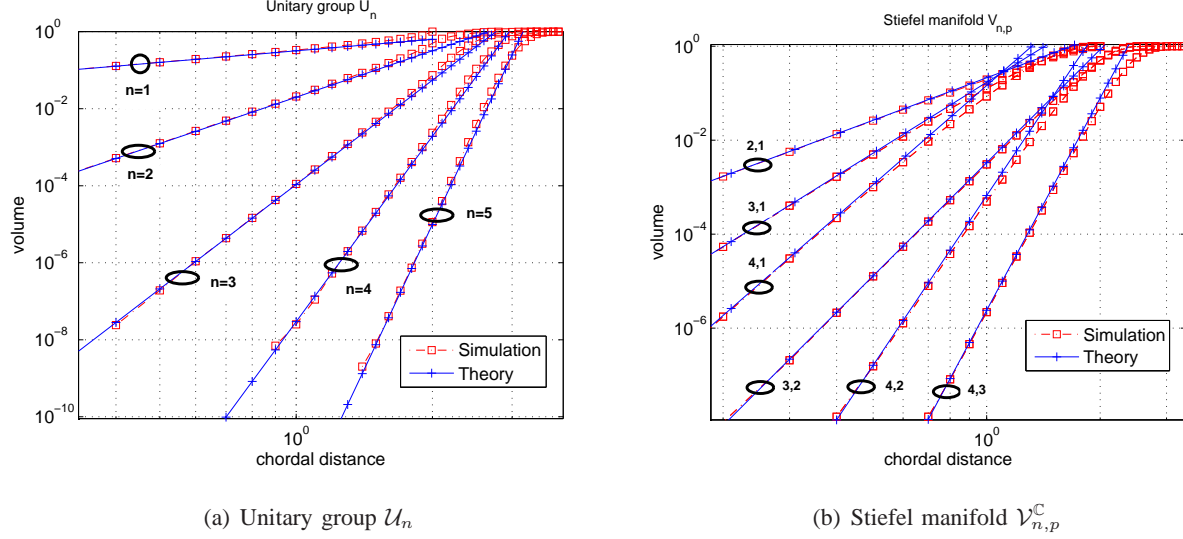


Fig. 1. The small ball volume approximation of Corollary 1 compared to simulation.

we have the following analogous result for the Stiefel and Grassmann manifolds, proved in Appendix C.

Lemma 2. *In the Stiefel manifold $(\mathcal{V}_{n,p}^C, d_c)$,*

$$\mu(B(r)) = 1 - \mu(B(\sqrt{4p - r^2})) \quad (44)$$

implying that the volume is symmetrical at $\mu(B(\sqrt{2p})) = 1/2$.

For the Grassmann manifold $(\mathcal{G}_{n,p}^C, d_c)$,

$$\mu(B(r)) = 1 - \mu\left(B_{\perp}\left(\sqrt{\frac{2p(n-p)}{n} - r^2}\right)\right), \quad (45)$$

where $B_{\perp}(\gamma) = \{[P] \in \mathcal{G}_{n,p}^C \mid d_c([Q], [P]) \leq \gamma\}$ for an arbitrary center $[Q] \in \mathcal{G}_{n,n-p}^C$ and with chordal distance¹ as defined in (19).

We remark that there is a structural difference here between the Stiefel and Grassmann manifolds. The antipodal on the embedding sphere to a point in the Stiefel manifold always belongs to the same Stiefel manifold. This is not always true for the Grassmann manifold except for $p = n/2$, as the antipodal on the sphere to a point in $\mathcal{G}_{n,p}^C$ belongs to $\mathcal{G}_{n,n-p}^C$. This observation will be useful in the interpretation of the high-dimensional regime discussed next.

¹Note here that the definition of the chordal distance between two Grassmannian planes of different dimensions is different than in [24], where then one would have $\mu(B(r)) = 1 - \mu(B_{\perp}(\sqrt{p - r^2}))$, see [29].

D. Volume Comparison Theorem and Spherical-Cap Approximation

We now present a second volume approximation: For the manifolds \mathcal{M} isometrically embedded in $\mathcal{S}^D(R)$, the uniform measure of a ball in \mathcal{M} can be well approximated by the spherical measure of a cap on $\mathcal{S}^D(R)$. The two normalized volumes are indeed asymptotically equivalent in the high-dimensional regime. Before stating the theorem, we highlight an intermediate result of independent interest.

Lemma 3. *The squared chordal distance of a uniformly distributed random point $\mathbf{Y} \in \mathcal{V}_{n,p}^{\mathbb{C}}$ from a reference point, say $\mathbf{I}_{n,p}$, converges in distribution to a Gaussian random variable*

- for the Stiefel manifold $\mathcal{V}_{n,p}^{\mathbb{C}}$ as $n \rightarrow \infty$,

$$d_c^2(\mathbf{I}_{n,p}, \mathbf{Y}) \xrightarrow{d} \mathcal{N}\left(2p, \frac{2p}{n}\right) \quad (46)$$

- for the Grassmann manifold $\mathcal{G}_{n,p}^{\mathbb{C}}$ as $n, p \rightarrow \infty$ with fixed $n - 2p$,

$$d_c^2([\mathbf{I}_{n,p}], [\mathbf{Y}]) \xrightarrow{d} \mathcal{N}\left(\frac{p(n-p)}{n}, \frac{p^2(n-p)^2}{n^4 - n^2}\right). \quad (47)$$

The proofs are given in Appendix D. It is obtained by reducing the chordal distances to the linear statistics of some random matrix ensembles and studying their moment-generating functions. Such linear statistics are asymptotically Gaussian, and by computing the two first moments one finds the asymptotic forms. The case of the Stiefel manifold is closely related to the partition function of the von-Mises Fisher distribution, while for the Grassmann manifold it is related to the partition function of the Bingham distribution [48].

The resulting volume comparison of the ball with the embedding spherical cap is given by

Theorem 2. *The normalized volume of a ball of radius r in \mathcal{M} is asymptotically equal to the volume of a cap of same radius in its embedding sphere $(\mathcal{M}, d_c) \hookrightarrow \mathcal{S}^{D-1}(R)$,*

$$\mu(B(r)) \simeq \sigma(C_{D,R}(r)), \quad (48)$$

when $n \rightarrow \infty$ for $\mathcal{M} = \mathcal{V}_{n,p}^{\mathbb{C}}$, and $n, p \rightarrow \infty$ with fixed $n - 2p$ for $\mathcal{M} = \mathcal{G}_{n,p}^{\mathbb{C}}$. Precisely, the volumes are asymptotically equal to (33)

- for the Stiefel manifold $\mathcal{V}_{n,p}^{\mathbb{C}}$,

$$\mu(B(r)) \simeq \frac{1}{2} \operatorname{erf}(\sqrt{np}) - \frac{1}{2} \operatorname{erf}\left(\sqrt{np} \left(1 - \frac{r^2}{2p}\right)\right), \quad (49)$$

- and for the Grassmann manifold $\mathcal{G}_{n,p}^{\mathbb{C}}$,

$$\mu(B(r)) \simeq \frac{1}{2} \operatorname{erf}\left(\sqrt{\frac{n^2 - 1}{2}}\right) - \frac{1}{2} \operatorname{erf}\left(\sqrt{\frac{n^2 - 1}{2}} \left(1 - \frac{n r^2}{p(n - p)}\right)\right). \quad (50)$$

The proof is given in Appendix E. The volume (49) generalizes our previous result [29], [30] from the unitary group to the Stiefel manifold. The volume (50) corresponds to the special case $p = q$ in [31]. Theorem 2 provides a geometric unification of the asymptotic expressions which are shown to be closely related due to their spherical embedding. The different asymptotic regimes for the Stiefel and Grassmann manifolds can be geometrically understood as the behaviors in Lemma 2. The Stiefel manifold fully covers all possible distances on its embedding sphere. This is not the case for the Grassmann manifold, and as a consequence $\mu(B(r))$ and $\sigma(C_{D,R}(r))$ are not defined on the same support, except for $\mathcal{G}_{n,\frac{n}{2}}^{\mathbb{C}}$. In the regime $n, p \rightarrow \infty$ with fixed $n - 2p$, one has $p \rightarrow \frac{n}{2}$ and the volume expressions are then asymptotically defined on the same support.

There exists a body of literature on comparison theorems in Riemannian geometry that compares volumes among manifolds with reference to the standard sphere. However, these theorems often compare manifolds of equal dimension, e.g. the Bishop-Gromov inequality or the Berger-Kazdan comparison theorem. To the best of our knowledge, volume comparisons of these manifolds with their embedding spheres in Theorem 2 is new.

The quality of the approximation is illustrated in Figure 2. The normalized volume of metric balls for different Grassmann and Stiefel manifolds obtained via Monte Carlo simulations is compared to the normalized volume of their respective embedding hyperspherical cap, together with their joint asymptotic expression. The exact volume of the hyperspherical cap is as given by Lemma 1. This numerical evaluation shows that the three volume expressions are very close to each other even in the low dimensional regime.

V. KISSING RADIUS AND DENSITY

In this section, we discuss the kissing radius of codes with chordal distance, and apply volume approximations derived in the previous section to evaluate code density. Recall that for the Grassmann and Stiefel manifold with chordal distance, the kissing radius ϱ cannot be directly expressed in term of the minimum distance of the code. In the following, upper and lower bounds on ϱ and the corresponding bounds on density are provided.

A. Preliminaries

1) *Hypothetical Covering Radius:* Ideally, a set of packing balls would fully cover the space, reaching a maximum density of one. It is in fact only possible when the cardinality of the code is $N = 2$, otherwise it provides an upper bound. This ideal radius r_N is the solution of the following equation

$$\mu(B(r_N)) = \frac{1}{N}. \quad (51)$$

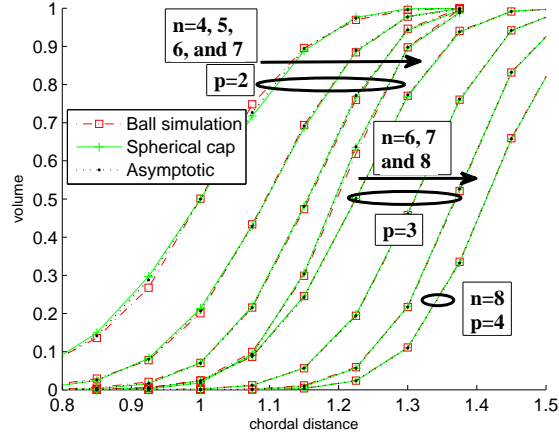
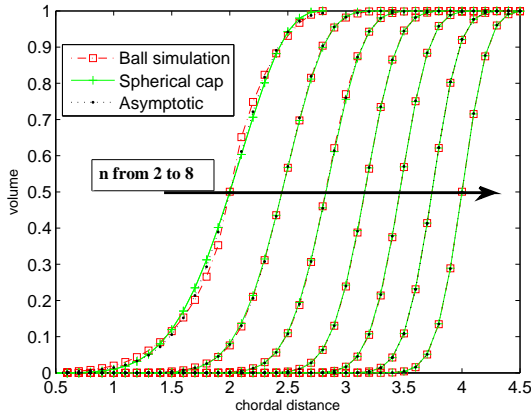
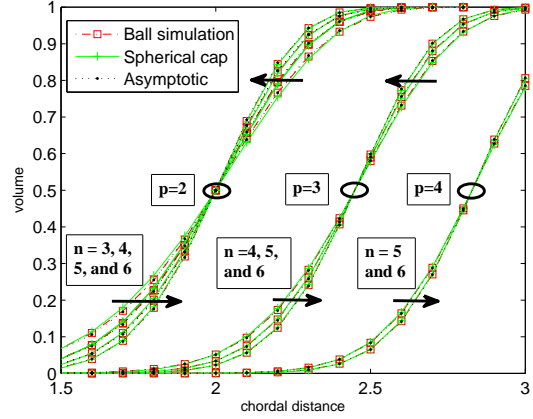
(a) Grassmann manifold $\mathcal{G}_{n,p}^C$ (b) Unitary group \mathcal{U}_n (c) Stiefel manifold $\mathcal{V}_{n,p}^C$

Fig. 2. Illustration of Theorem 2: spherical cap volume, volume of balls in manifolds (Monte Carlo simulation), and asymptotic evaluation.

Two volume approximations were discussed in the previous section, and depending of the regime, one may compute r_N accordingly.

- For N sufficiently large, namely $N \geq c_{n,p}^{-1}$ to guarantee a radius less than one, the small ball approximation leads to

$$r_N \approx (c_{n,p} N)^{\frac{-1}{\dim}}, \quad (52)$$

where $c_{n,p}$ is given in Corollary 1 and \dim is the dimension of the manifold as given in Table I.

- Otherwise for a larger ball, occurring with n, p large and relatively small N , the spherical approxi-

mation of Theorem 2 leads to

$$r_N \approx \sqrt{2}R \sqrt{1 - \sqrt{\frac{2}{D}} \operatorname{erf}^{-1} \left(\operatorname{erf} \sqrt{\frac{D}{2}} - \frac{2}{N} \right)}, \quad (53)$$

where R, D are the radius and the dimension of the spherical embedding, provided in Table I.

2) *Kissing Radius for Spherical Codes*: For spherical codes with chordal distance, the kissing radius of a code is a one-to-one mapping from its minimum distance, directly computable by Pythagorean theorem. Given an (N, δ) -spherical code on $\mathcal{S}^{D-1}(R)$, the midpoint on the geodesic between the two codewords of distance δ is at distance ϱ_s from the extremities:

$$\varrho_s = \sqrt{2}R \sqrt{1 - \sqrt{1 - \frac{\delta^2}{4R^2}}}, \quad (54)$$

which can be inverted as

$$\delta^2 = 4\varrho_s^2 - \frac{\varrho_s^4}{R^2}. \quad (55)$$

3) *Preliminary Bounds on Kissing Radius*: Since we are considering a manifold isometrically embedded in the Euclidean sphere $\mathcal{S}^{D-1}(R)$, an (N, δ) -code in \mathcal{M} is a (N, δ) -spherical code. As a consequence, as balls of radius ϱ_s are non-overlapping on $\mathcal{S}^{D-1}(R)$, their inverse image on \mathcal{M} are also non-overlapping, and we can deduce that $\varrho_s \leq \varrho$. On the other hand, we know that for every non-overlapping ball of radius r , we have $r \leq r_N$.

Lemma 4. *Given an (N, δ) -code in \mathcal{M} isometrically embedded in $\mathcal{S}^{D-1}(R)$, the kissing radius ϱ is bounded by*

$$\varrho_s \leq \varrho \leq r_N, \quad (56)$$

where ϱ_s is given in (54) and r_N satisfies (51).

It should be noted here that the lower bound is a function of the minimum distance δ , while the upper bound is a function of the cardinality N .

B. Bounds on Kissing Radius and Density

We now provide bounds on the kissing radius as a function of the minimum distance of the code only, and corresponding bounds on code density.

Proposition 1. *For any (N, δ) -code \mathcal{C} in \mathcal{M} , we have*

$$\underline{\varrho} \leq \varrho_c \leq \bar{\varrho}, \quad (57)$$

where

$$\underline{\varrho} = \begin{cases} \sqrt{\frac{p}{2} \left(1 - \sqrt{1 - \frac{\delta^2}{p}}\right)} & \text{for } \mathcal{M} = \mathcal{G}_{n,p}^{\mathbb{C}} \\ \sqrt{2p \left(1 - \sqrt{1 - \frac{\delta^2}{4p}}\right)} & \text{for } \mathcal{M} = \mathcal{V}_{n,p}^{\mathbb{C}} \end{cases} \quad (58)$$

$$\bar{\varrho} = \begin{cases} \frac{1}{\sqrt{2}} \sqrt{\lceil \delta^2 \rceil - \sqrt{\lceil \delta^2 \rceil - \delta^2}} & \text{for } \mathcal{M} = \mathcal{G}_{n,p}^{\mathbb{C}} \\ \sqrt{2} \sqrt{\lceil \frac{\delta^2}{4} \rceil - \sqrt{\lceil \frac{\delta^2}{4} \rceil - \frac{\delta^2}{4}}} & \text{for } \mathcal{M} = \mathcal{U}_n \end{cases} \quad (59)$$

and $\lceil x \rceil$ is the smallest integer greater than x . It follows, therefore, that the density is bounded by

$$N\mu(B(\underline{\varrho})) \leq \Delta(\mathcal{C}) \leq \min\{1, N\mu(B(\bar{\varrho}))\}. \quad (60)$$

A detailed proof can be found in Appendix F. Given two points either on the Grassmann manifold or the unitary group, their midpoint can be determined according to their principal angles. The bounds then follow by optimizing over the principal angles. For the unitary group, the obtained lower bound is matching the spherical lower bound in Lemma 4, and can thus be extended to any Stiefel manifold. While it is very likely that the upper bound (59) could be generalized to all Stiefel manifolds, the lack of precise geodesic equation between two points, as explained in Remark 1 (or equivalently the absence of notion of principal angles), renders a tentative proof of generalization difficult. We remark nevertheless that numerical experiments support a putative generalization, and that the upper bounds (59) do not depend on any dimension parameter.

For the Grassmann manifold, the lower bound in Proposition 1 provides an improvement of the spherical embedding bound (see Appendix F-D).

Corollary 2. *For the Grassmann manifold, the lower bound in Proposition 1 is tighter than the lower bound in Lemma 4. These two bounds are equal if and only if $p = n/2$.*

Figure 3 illustrates the upper and lower bounds (57) on the kissing radius and shows that $\delta/2$ is a good approximation for ϱ only when the minimum distance of the code is relatively small. In general, since the chordal distance is not strictly intrinsic, we have $\frac{\delta}{2} < \varrho$. The bounds are also compared to 10^5 simulated midpoints between a fixed center and uniformly-distributed random points. We stress that in this case the bounds are tight in the sense that it is always possible to construct two diagonal codewords fulfilling the bounds.

Figure 4 compares the density of codes with sizes from $N = 2$ to $N = 15$ in $\mathcal{G}_{4,2}^{\mathbb{C}}$ to the density bounds in Proposition 1. The Grassmannian $\mathcal{G}_{4,2}^{\mathbb{C}}$ is embedded in $\mathcal{S}^{14}(\frac{1}{\sqrt{2}})$. Accordingly, the spherical Rankin

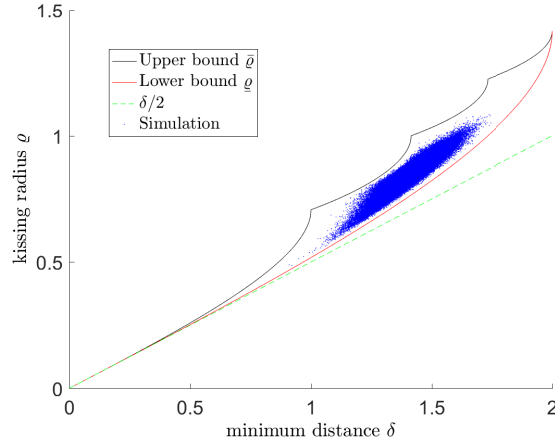
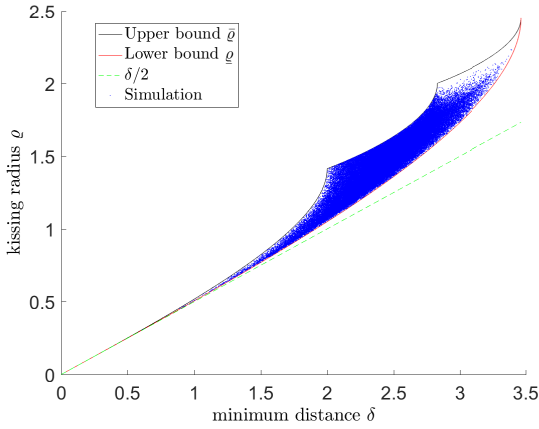
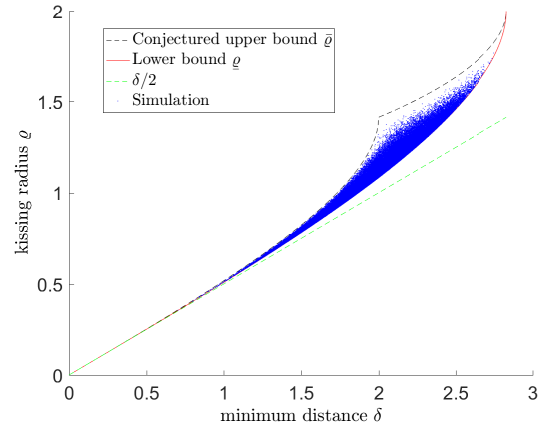
(a) Grassmann manifold $\mathcal{G}_{8,4}^C$ (b) Unitary group \mathcal{U}_3 (c) Stiefel manifold $\mathcal{V}_{4,2}^C$

Fig. 3. Illustration of the kissing radius bounds from Proposition 1. Bounds are compared to simulated midpoints between two randomly generated codewords. It is also compared with the estimate $\delta/2$, corresponding to the classical packing radius in flat geometry.

bound applies² providing an upper bound on the maximum possible minimum distance of Grassmannian codes. We generated Grassmannian codes according to two criteria: maximum-minimum-distance codes and low-distortion³ codes from Lloyd algorithm. For visibility, the densities from the latter are displayed at $(N + 0.1)$ while for the former at $(N - 0.1)$. The bounds from Proposition 1 are shown with error bars. The higher is the minimum distance of the code, the higher is the bar.

²In this dimensionality, spherical codes achieve the simplex bound for $N \leq 15$, then the orthoplex bound for $16 \leq N \leq 30$.

³The code distortion refers here to the average squared quantization error of a uniform random source quantized to the code.

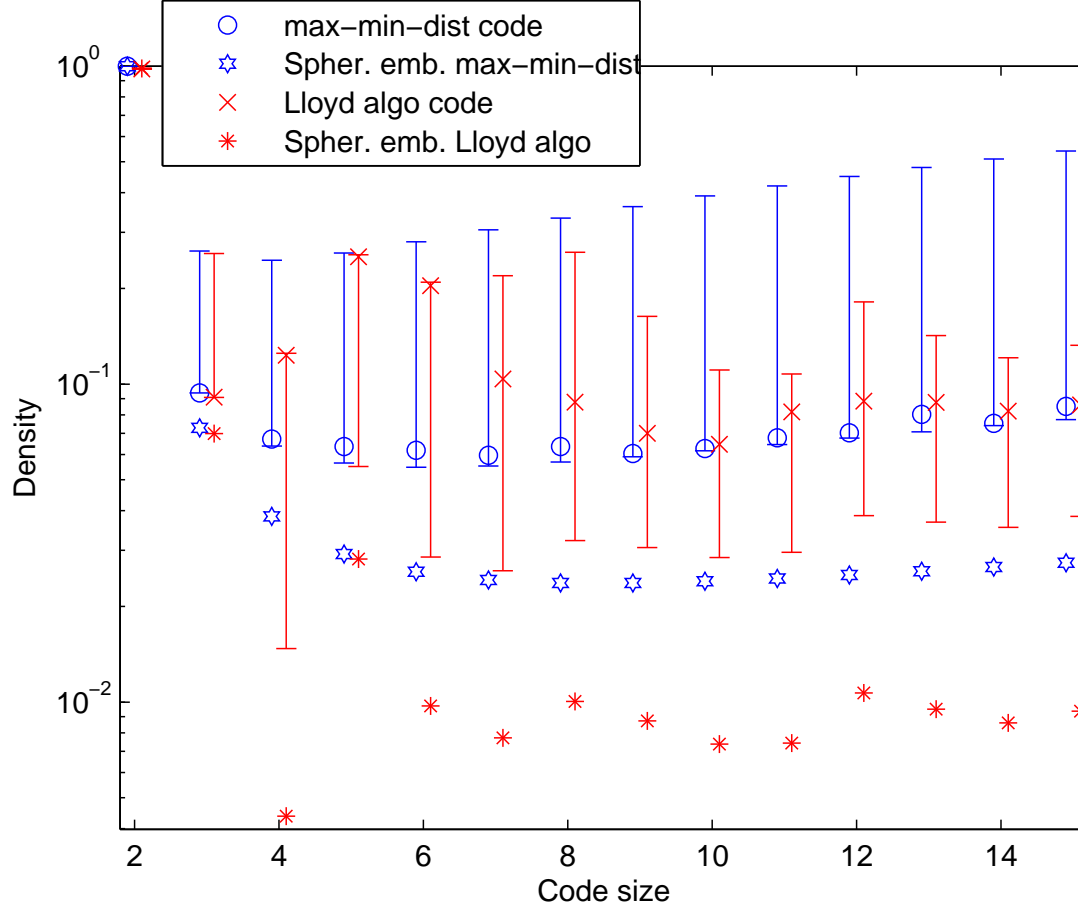


Fig. 4. Density of codes in $\mathcal{G}_{4,2}^C$ and their image code in $S^{14}(\frac{1}{\sqrt{2}})$ as a function of the number of points. The error bars represent the density bounds from Proposition 1 obtained according to their minimum distance.

Maximum-minimum-distance codes for $N < 15$ were obtained using the Alternating Projection algorithm from [39]. The obtained codes were matching the Rankin bound on squared minimum distance with 10^{-4} numerical precision⁴.

On the other hand, we expected the Lloyd algorithm to provide good code density since the kissing radius corresponds to the first border effect of Voronoi cells. In [24], it was shown that codes' distortions are bounded by idealized codes that would have only one border effect, corresponding to a kissing radius equal to r_N , i.e. the upper bound of Lemma 4.

While the Alternating Projection algorithm generates numerically optimal simplicial codes with maximum minimum distance, their density appears to be always close to the corresponding lower bound.

⁴The recorded values here are actually better than in [39] due to a higher number of iterations: 10^5 .

This means that the codes are strongly simplicial configurations where all principal angles exhibit similar values. Comparing to the codes generated by Lloyd algorithm, the results for cardinalities 3, 4 and 5 are instructive on the weak relationship between maximizing the minimum distance and maximizing the density. For $N = 3$, the Lloyd algorithm produced a similar max-min-distance code reaching also the density lower bound. For $N = 4$, it generated a code with much smaller minimum distance but much larger density reaching its upper bound. The configurations obtained for $N = 4$ correspond to codes numerically equivalent to the analytical ones in Table II. For $N = 5$, the Lloyd algorithm produced a code with minimum distance close to the optimum, as for $N = 3$, but this time with a density reaching the upper bound, while the code from the Alternating Projection algorithm is close to the lower bound. For other cardinalities, the Lloyd algorithms produced in general codes with greater or equal density but smaller minimum distance than Alternating-Projection codes.

Lastly, an interesting specificity of Grassmann codes is that their density for $N = 2$ is not $\Delta = 1$, except for $p = \frac{n}{2}$. This comes from the fact that when $p \neq \frac{n}{2}$ one cannot have two spherically antipodal points, c.f. the symmetry of Lemma 2. For example, the density of two orthogonal lines in $\mathcal{G}_{3,1}^C$ is equal to 0.5, and one can actually pack a third orthogonal line to reach the density of 0.75.

C. Relation to Density of Spherical Codes.

As considered in this work, for manifolds isometrically embedded in Euclidean spheres, an (N, δ) -code in \mathcal{M} is also an (N, δ) -spherical code. The density of a code in the manifold differs from the density of its image code in the embedding sphere. Combining the asymptotic equality from Theorem 2 between volume of balls in the manifold and hyperspherical cap with the kissing radius bounds from Proposition 1, we have the following comparison.

Proposition 2. *The density of codes in the Stiefel and Grassmann manifolds are asymptotically greater than the density of their image spherical codes in the high-dimensional regime of Theorem 2. The inequality is strict for the Grassmann manifold with $N > 2$.*

This proposition is illustrated in Figure 4 where densities of the image spherical codes of the considered Grassmann codes are also depicted. One observes that the densities of the image spherical codes are always less than the densities of the original Grassmannian codes for $N > 2$.

We remark also few special cases. In the case $p = 1$, the lower and upper bounds on the kissing radius in Proposition 1 are matching $\varrho = \bar{\varrho}$. Moreover with $p = 1$, the Stiefel manifold is isometric to the embedding sphere, while for the Grassmann manifold the volume of a ball has been calculated exactly

in [24]. In these cases the density can be computed exactly as a function of the minimum distance.

Corollary 3. *For any packing with $p = 1$, on manifolds $\mathcal{G}_{n,1}^{\mathbb{C}}$ or $\mathcal{V}_{n,1}^{\mathbb{C}}$,*

$$\varrho = \underline{\varrho} = \bar{\varrho} \quad (61)$$

and

$$\Delta(\mathcal{C}) = \begin{cases} N \left(\frac{1-\sqrt{1-\delta^2}}{2} \right)^{n-1} & \text{for } \mathcal{M} = \mathcal{G}_{n,1}^{\mathbb{C}} \\ NI_{\frac{1}{2}(1-\sqrt{1-\delta^2/4})} \left(\frac{2n-1}{2}, \frac{2n-1}{2} \right) & \text{for } \mathcal{M} = \mathcal{V}_{n,1}^{\mathbb{C}} \end{cases}. \quad (62)$$

Finally, for the specific case of $n = 2$, $p = 1$, the Grassmann manifold is also isometric to the real sphere: $\mathcal{G}_{2,1}^{\mathbb{C}} \cong S^2$ [49, Ex. 17.23] [40], and the discussed definition of the density of a code is consistent with the definition of the density for a sphere packing as defined previously in the literature [50].

D. Hamming-type Bounds

Bounds on density directly translate to Hamming-type bounds on the code's cardinality and minimum distance.

1) *Hamming Bound on Cardinality:* According to Proposition 1, we have the following:

Corollary 4. *For any (N, δ) -code in \mathcal{M} , and given $\underline{\varrho}$ defined in (58),*

$$N \leq \frac{1}{\mu(B(\underline{\varrho}))}. \quad (63)$$

This bound is equivalent to the one derived in [17] for the unitary group. For the Grassmann manifold, this provides an improved bound compared to the sphere embedding argument used for asymptotical analysis in [19].

2) *Hamming-type Bound on Minimum Distance:* From the spherical embedding of the manifolds, we have the following Hamming-type bound on the minimum distance:

Lemma 5. *Given an (N, δ) -code in \mathcal{M} isometrically embedded in $S^{D-1}(R)$, and a r_N satisfying (51), we have*

$$\delta^2 \leq 4r_N^2 - \frac{r_N^4}{R^2}. \quad (64)$$

This follows from a direct combination of (55) and Lemma 4. A similar bound was derived for the unitary group in [17, Theorem 2.4]. For the Stiefel manifold, the result is new. For the Grassmann manifold, a tighter bound is provided as a by-product of Proposition 1, which is a generalization of a bound for line packing in [51] to any value of p .

Lemma 6. *Given a (N, δ) -code in $\mathcal{G}_{n,p}^{\mathbb{C}}$, one must satisfy*

$$\delta^2 \leq 4r_N^2 - \frac{4}{p}r_N^4. \quad (65)$$

Remark 2. *For the case $p = 1$ the bound of Lemma 6 reduces to the following bound derived in [51, (32)]:*

$$\delta^2 \leq 4N^{\frac{-1}{n-1}} - 4N^{\frac{-2}{n-1}}. \quad (66)$$

3) *Illustration and Conjectured Improvement:* The standard Hamming bound (27) and the Hamming bound from the kissing radius analysis (65) are displayed in Fig. 5 for the Grassmannian $\mathcal{G}_{4,2}^{\mathbb{C}}$ as a function of the code rate. One verifies that (65) improves (27) and they are getting equivalent as $N \rightarrow \infty$. These Hamming bounds are also compared to the Rankin bound. For $\mathcal{G}_{4,2}^{\mathbb{C}}$, the Rankin bound is tight at the saturating value $N = 30$ [52], i.e. at rate 1.22. For higher cardinality the Rankin bound is not reachable. As expected, the Hamming bounds are tighter than the Rankin bound for large code sizes.

By construction the Hamming bound is loose even if one would be able to exactly compute the kissing radius ϱ as a function of minimum distance. The manifold can never be totally covered by packing balls (except for $N = 2$), and one always has a gap between ϱ and r_N . In order to sharpen the Hamming bound one could use $\bar{\varrho}$ rather than ϱ to get a better estimate of the minimum distance. It is very likely that in general $\bar{\varrho} \leq r_N$, which can be verified at the two ends of the code size spectrum $N = 2$ and $N \rightarrow \infty$. Inverting (59) gives the following approximation,

$$\delta^2 \lesssim \begin{cases} \lceil 2r_N^2 \rceil - (\lceil 2r_N^2 \rceil - 2r_N^2)^2 & \text{for } \mathcal{M} = \mathcal{G}_{n,p}^{\mathbb{C}} \\ 4\lceil \frac{r_N^2}{2} \rceil - 4(\lceil \frac{r_N^2}{2} \rceil - \frac{r_N^2}{2})^2 & \text{for } \mathcal{M} = \mathcal{U}_n \end{cases}, \quad (67)$$

which is guaranteed to be an upper bound as $N \rightarrow \infty$. This conjectured improvement is displayed for $\mathcal{G}_{4,2}^{\mathbb{C}}$ in Fig. 5. Interestingly, it meets the Rankin bound at $N = 32$, i.e. close to $N = 30$ where the Rankin bound is saturating.

VI. CONCLUSION

The density of Grassmann and Stiefel codes with chordal distance has been investigated. The analysis pertains to treat the codes as subclasses of spherical codes since the chordal distance induces embeddings in Euclidean hyperspheres. The investigation is motivated by an exotic behavior: in this context maximizing codes' density is not equivalent to maximizing codes' minimum distance. We addressed both critical steps to compute a code's density, which are computing the volume of balls and the kissing radius. For the volume of balls, our main results included a proper scaling of the manifolds' volume consistent with the

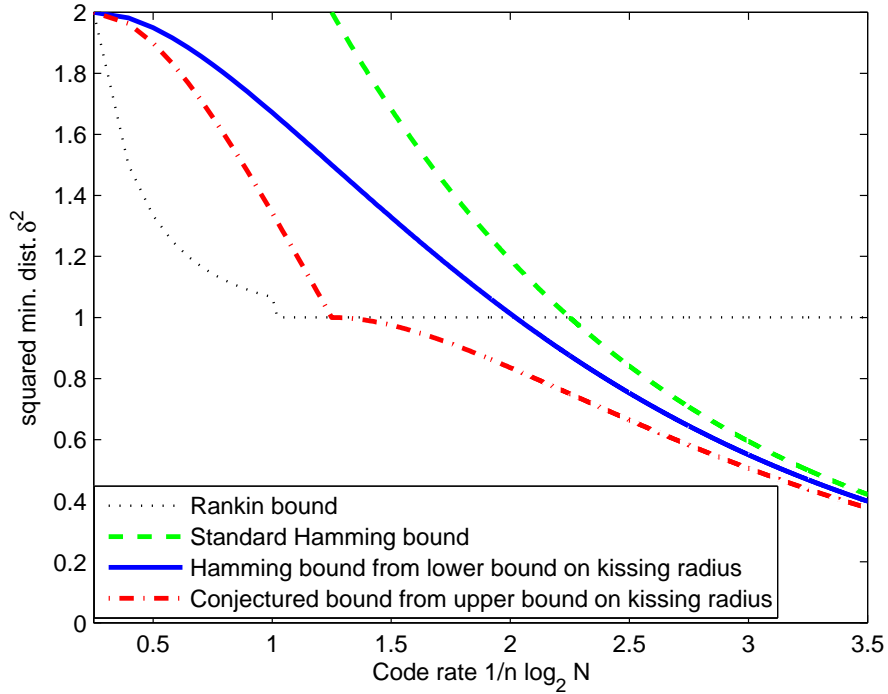


Fig. 5. The standard Hamming bound (27), the Hamming bound from the kissing radius analysis (65) and a conjectured improvement (67), compared to the Rankin bound for codes in $\mathcal{G}_{4,2}^C$.

distance, which are needed in small ball approximation. It included moreover the asymptotic Gaussian behavior of chordal distances in the high-dimensional regime leading to the asymptotic equivalence between the volume of balls in the manifolds and the volume of caps in the embedding spheres. Then the kissing radius and density of codes were bounded as a function of the minimum distance of the codes. It was concluded that Stiefel and Grassmann codes have larger density than their image spherical codes in high dimensions. Finally, as a by-product of the analysis, refinements of the standard Hamming bounds for Stiefel and Grassmann codes were provided.

APPENDIX A

PROOF OF LEMMA 1–HYPERSPHERICAL CAP AREA

A. Proof of (31)

The area of a hyperspherical cap is given in [53] in which the radius of the cap is measured by an angle $0 \leq \phi \leq \frac{\pi}{2}$. This translates in our notation to a radius of $r^2 = 2R^2(1 - \cos \phi)$, that gives

$\sin^2 \phi = \frac{r^2}{R^2}(1 - \frac{r^2}{4R^2})$ and directly leads to

$$\text{vol}(C_{D,R}(r)) = \frac{A_D(R)}{2} I_{\frac{r^2}{R^2}(1 - \frac{r^2}{4R^2})} \left(\frac{D-1}{2}, \frac{1}{2} \right) \quad (68)$$

for $r \leq \sqrt{2}R$.

The result further simplifies by normalizing by the overall area of the sphere $A_D(R)$ and using the identity $I_x(a, a) = \frac{1}{2} I_{4x(1-x)}(a, \frac{1}{2})$ valid for $0 \leq x \leq \frac{1}{2}$ [54, (8.17.6)] [55]. The volume for larger radius $r \geq \sqrt{2}R$ can be computed by the complementary cap, i.e.

$$\sigma(C_{D,R}(r)) = 1 - \sigma(C_{D,R}(\sqrt{4R^2 - r^2})), \quad (69)$$

and using the identity $I_x(a, b) = 1 - I_{1-x}(b, a)$ [54, (8.17.4)] [55]. Altogether, one obtains (31) for the whole range of the radius $0 \leq r \leq 2R$.

B. Proof of (32) – Small Cap

We start from (68) which after normalization gives

$$\sigma(C_{D,R}(r)) = \frac{1}{2} I_{\frac{r^2}{R^2}(1 - \frac{r^2}{4R^2})} \left(\frac{D-1}{2}, \frac{1}{2} \right). \quad (70)$$

Expressing the regularized incomplete beta function $I_x(a, b) = B_x(a, b)/B(a, b)$ with the Beta function $B(a, b) = \Gamma(a)\Gamma(b)/\Gamma(a+b)$ and the incomplete Beta function $B_x(a, b)$ gives

$$\sigma(C_{D,R}(r)) = \frac{1}{2\sqrt{\pi}} \frac{\Gamma(\frac{D}{2})}{\Gamma(\frac{D-1}{2})} B_{\frac{r^2}{R^2}(1 - \frac{r^2}{4R^2})} \left(\frac{D-1}{2}, \frac{1}{2} \right). \quad (71)$$

From the identity $B_x(a, b) = \frac{x^a}{a} F(a, 1-b; a+1; x)$ [54, (8.17.7)] where $F(a, b; c; z)$ is the hypergeometric function given by [54, (15.2.1)], it can be verified that $B_x(a, b) = \frac{x^a}{a}(1 + O(x))$ as $x \rightarrow 0$, which in turn gives

$$\lim_{r \rightarrow 0} \sigma(C_{D,R}(r)) = \frac{1}{2\sqrt{\pi}} \frac{\Gamma(\frac{D}{2})}{\Gamma(\frac{D+1}{2})} \frac{r^{D-1}}{R^{D-1}} (1 + O(r^2)). \quad (72)$$

C. Proof of (33) – Large Dimension

The normalized volume of a cap $C_{D,R}(r)$ can be interpreted as the probability that a uniformly distributed vector $\mathbf{x} \in \mathcal{S}^{D-1}(R)$ is at distance less than r from a fixed point \mathbf{e} . The volume is reformulated as

$$\begin{aligned} \sigma(C_{D,R}(r)) &= \Pr\{\mathbf{x} \mid 0 \leq d_c(\mathbf{e}, \mathbf{x}) \leq r\} \\ &= F_{d_c^2}(r^2) - F_{d_c^2}(0), \end{aligned} \quad (73)$$

where $F_{d_c^2}(z)$ is the cumulative distribution of the random variable $d_c^2(\mathbf{e}, \mathbf{x})$.

Without loss of generality, one can choose the center to be $\mathbf{e} = [1, 0, \dots, 0]^T$ so that the distance is $d_c^2(\mathbf{e}, \mathbf{x}) = 2R^2(1 - x_1)$ where x_1 is the first coordinate of \mathbf{x} . As $D \rightarrow \infty$, the coordinate x_1 converges in distribution to a Gaussian random variable, $x_1 \rightarrow \mathcal{N}(0, \frac{1}{D})$ [32], [33]. It follows that $d_c^2(\mathbf{e}, \mathbf{x}) \rightarrow \mathcal{N}(2R^2, \frac{4R^4}{D})$ in distribution, i.e.

$$F_{d_c^2}(z) \rightarrow \frac{1}{2} \left(1 + \operatorname{erf} \left(\sqrt{\frac{D}{2}} \left(\frac{z}{2R^2} - 1 \right) \right) \right), \quad (74)$$

where

$$\operatorname{erf}(x) = \frac{2}{\sqrt{\pi}} \int_0^x e^{-t^2} dt \quad (75)$$

is the Gauss error function. The final expression is obtained after some straightforward algebraic manipulations.

APPENDIX B

PROOFS OF OVERALL VOLUMES

In general, if \mathcal{M} is an m -dimensional Riemann manifold with infinitesimal metric form

$$ds^2 = \sum_{j,k=1}^m g_{jk} dx_j dx_k \quad (76)$$

in local coordinates $\{x_j\}_{j=1}^m$. The volume element of \mathcal{M} is [56]

$$d\omega = \sqrt{\det\{g_{jk}\}_{j,k=1}^m} dx_1 \dots dx_m. \quad (77)$$

Now, consider the Euclidean space of $m \times m$ complex matrices with its canonical inner product $(\mathbb{C}^{m \times m}, \langle \cdot, \cdot \rangle = \Re \operatorname{Tr} \cdot^H)$ from which the Riemann metrics considered are constructed. Given $\mathbf{M} \in \mathbb{C}^{m \times m}$ we have

$$\begin{aligned} ds^2 &= \Re \operatorname{Tr}(d\mathbf{M}^H d\mathbf{M}) = \|d\mathbf{M}\|_F^2 \\ &= \sum_{j,k=1}^m \Re(d\mathbf{M}_{jk})^2 + \Im(d\mathbf{M}_{jk})^2. \end{aligned} \quad (78)$$

Restricting the metric to the space of skew-Hermitian matrix, with $\mathbf{A} \in \mathfrak{u}(m)$ we get

$$ds_{\mathbf{A}}^2 = -\operatorname{Tr}(d\mathbf{A}^2) = \sum_{j=1}^m |d\mathbf{A}_{jj}|^2 + 2 \sum_{j < k} |d\mathbf{A}_{jk}|^2 \quad (79)$$

and the corresponding volume element

$$d\omega_{\mathbf{A}} = 2^{\frac{m(m-1)}{2}} \prod_{j=1}^m |d\mathbf{A}_{jj}| \prod_{j < k} \Re(d\mathbf{A}_{jk}) \Im(d\mathbf{A}_{jk}). \quad (80)$$

Note here that the off-diagonal elements are counted twice, leading to an overall scaling factor of $2^{\frac{m(m-1)}{2}}$. The overall volumes of the manifolds need to be scaled accordingly to be consistent with the chosen metric.

A. Volume of Unitary Group

Given a unitary matrix $U \in \mathcal{U}_n$, by differentiating $U^H U = I$, we obtain

$$U^H dU + dU^H U = 0 \quad (81)$$

showing that the differential form $U^H dU$ is skew-Hermitian. Due to the unitary invariance of the metric ds^2 , its restriction to \mathcal{U}_n can be expressed in terms of the global form $U^H dU$. Then, the infinitesimal metric is

$$ds_U^2 = -\text{Tr}(U^H dU)^2 = \sum_{j=1}^n |(U^H dU)_{jj}|^2 + 2 \sum_{j < k} |(U^H dU)_{jk}|^2 \quad (82)$$

and the volume form in local coordinates is

$$d\omega_U = 2^{\frac{n(n-1)}{2}} d\nu_U, \quad (83)$$

where

$$d\nu_U = \prod_{j=1}^n |(U^H dU)_{jj}| \prod_{j < k} \Re((U^H dU)_{jk}) \Im((U^H dU)_{jk}) \quad (84)$$

is a common volume element normalized so that $\int_{\mathcal{U}_n} d\nu_U = \frac{2^n \pi^{n^2}}{\tilde{\Gamma}_n(n)}$ [57]. Finally with the metric considered,

$$\text{vol } \mathcal{U}_n = \frac{2^{\frac{n(n+1)}{2}} \pi^{n^2}}{\tilde{\Gamma}_n(n)}. \quad (85)$$

B. Volume for Stiefel Manifold in Theorem 1

Now let $Y \in \mathcal{V}_{n,p}^{\mathbb{C}}$ and $U \in \mathcal{U}_n$ such that $U^H Y = I_{n,p}$, i.e. the first p columns of $U = \begin{pmatrix} Y & Y^\perp \end{pmatrix}$ are the columns of Y . The differential form $U^H dY$ is “rectangular skew-Hermitian”, i.e. $U^H dY = \begin{pmatrix} Y^H dY \\ Y^{\perp H} dY \end{pmatrix}$ where $Y^H dY$ is p -by- p skew-Hermitian. Similarly, due to unitary invariance of the metric, the volume element for the Stiefel manifold can be expressed in terms of the global form $U^H dY$ and is given in local coordinates as

$$d\omega_Y = 2^{\frac{p(p-1)}{2}} d\nu_Y, \quad (86)$$

where

$$d\nu_Y = \prod_{i=1}^p |(U^H dY)_{ii}| \prod_{k=1}^p \prod_{j=k+1}^n \Re((U^H dY)_{jk}) \Im((U^H dY)_{jk}) \quad (87)$$

is a common volume element normalized so that $\int_{\mathcal{V}_{n,p}^{\mathbb{C}}} d\nu_{\mathbf{Y}} = \frac{2^p \pi^{np}}{\tilde{\Gamma}_p(n)}$ [57]. Finally,

$$\text{vol } \mathcal{V}_{n,p}^{\mathbb{C}} = \frac{2^{\frac{p(p+1)}{2}} \pi^{np}}{\tilde{\Gamma}_p(n)}. \quad (88)$$

C. Volume for Grassmann Manifold

The volume of the Grassmann manifold directly follows from the quotient geometry over the Stiefel manifold associated with d_g :

$$\text{vol } \mathcal{G}_{n,p}^{\mathbb{C}} = \frac{\text{vol } \mathcal{V}_{n,p}^{\mathbb{C}}}{\text{vol } \mathcal{U}_p}. \quad (89)$$

Alternatively it can be computed from the quotient geometry over the unitary group associated with d_{g*}

$$\text{vol } \mathcal{G}_{n,p}^{\mathbb{C}} = 2^{-\frac{\dim}{2}} \frac{\text{vol } \mathcal{U}_n}{\text{vol } \mathcal{U}_p \text{vol } \mathcal{U}_{n-p}}, \quad (90)$$

where the scaling coefficient comes from the $\sqrt{2}$ in the definition of d_{g*} compared to d_g .

APPENDIX C

PROOF OF LEMMA 2—COMPLEMENTARY BALLS

a) Stiefel Manifold: Consider the center to be $\mathbf{I}_{n,p} \in \mathcal{V}_{n,p}^{\mathbb{C}}$. It has a unique antipodal point (i.e. a furthest possible point away from $\mathbf{I}_{n,p}$) which is $-\mathbf{I}_{n,p}$ and we have

$$d_c(\mathbf{I}_{n,p}, -\mathbf{I}_{n,p}) = 2\sqrt{p} \triangleq d_{\max}. \quad (91)$$

Given a point $\mathbf{Y} \in \mathcal{V}_{n,p}^{\mathbb{C}}$ such that $d_c(\mathbf{I}, \mathbf{Y}) \geq r$, it is a direct verification that $d_c(-\mathbf{I}, \mathbf{Y}) \leq \sqrt{d_{\max}^2 - r^2}$, thus $\mathbf{Y} \notin B_{\mathbf{I}}(r)$ implies $\mathbf{Y} \in B_{-\mathbf{I}}(\sqrt{d_{\max}^2 - r^2})$ and finally

$$\mu(B(r)) + \mu(B(\sqrt{d_{\max}^2 - r^2})) = 1. \quad (92)$$

b) Grassmann Manifold: From the mapping (18), the Grassmann manifolds $\mathcal{G}_{n,p}^{\mathbb{C}}$ and $\mathcal{G}_{n,n-p}^{\mathbb{C}}$ are both embedded in the same sphere $\mathcal{S}^{n^2-2}(\sqrt{\frac{p(n-p)}{2n}})$. The definition of chordal distance thus directly extends between any $[\mathbf{Y}] \in \mathcal{G}_{n,p}^{\mathbb{C}}$ and $[\mathbf{Z}] \in \mathcal{G}_{n,n-p}^{\mathbb{C}}$ as

$$\begin{aligned} d_c^2([\mathbf{Y}], [\mathbf{Z}]) &= \|\bar{\Pi}_{\mathbf{Y}} - \bar{\Pi}_{\mathbf{Z}}\|_F^2 \\ &= \frac{2p(n-p)}{n} - \|\mathbf{Y}^H \mathbf{Z}\|_F^2 \end{aligned} \quad (93)$$

The distance reaches its maximum at $d_{\max} = \sqrt{\frac{2p(n-p)}{n}}$ with $[\mathbf{Z}] = [\mathbf{Y}_{\perp}]$, where the \mathbf{Y}_{\perp} is the orthogonal complement of \mathbf{Y} such that $\begin{pmatrix} \mathbf{Y} & \mathbf{Y}_{\perp} \end{pmatrix}$ is a unitary matrix. The maximum distance is exactly twice the embedding radius, $d_{\max} = 2R$, i.e. $[\mathbf{Y}_{\perp}]$ is the antipodal of $[\mathbf{Y}]$ on the embedding sphere. The final result follows by the same argumentation as for the Stiefel manifold. Here the Pythagorean theorem gives $d_c^2([\mathbf{Y}], [\mathbf{Z}]) + d_c^2([\mathbf{Y}_{\perp}], [\mathbf{Z}]) = \frac{2p(n-p)}{n}$.

APPENDIX D

PROOF OF THE ASYMPTOTIC GAUSSIANTY OF THE CHORDAL DISTANCES IN LEMMA 3

Before proceeding the proof, we first state some useful definitions and intermediary results.

A. The Hypergeometric Function of Complex Matrix Argument

For an $n \times n$ Hermitian matrix \mathbf{A} , the hypergeometric function of a complex matrix argument is defined as [58], [59]

$${}_p\tilde{F}_q(a_1, \dots, a_p; b_1, \dots, b_q; \mathbf{A}) = \sum_{k=0}^{\infty} \sum_{\kappa} \frac{(a_1)_{\kappa} \cdots (a_p)_{\kappa}}{(b_1)_{\kappa} \cdots (b_q)_{\kappa}} \frac{C_{\kappa}(\mathbf{A})}{k!}, \quad (94)$$

where κ denotes a partition of integer k into no more than n parts, i.e. $k = \kappa_1 + \kappa_2 + \cdots + \kappa_n$ with $\kappa_1 \geq \kappa_2 \geq \cdots \geq \kappa_n \geq 0$, and

$$(a)_{\kappa} = \prod_{j=1}^n (a - j + 1)_{\kappa_j} = \prod_{j=1}^n \frac{(\kappa_j + a - j)!}{(a - j)!} \quad (95)$$

is the multivariate hypergeometric coefficient [58, Eq. (84)]. In (94), $C_{\kappa}(\mathbf{A})$ denotes a zonal polynomial [58], [59], which is a homogenous symmetric polynomial of degree k in the n eigenvalues of \mathbf{A} . Denoting the j -th eigenvalue of \mathbf{A} by a_j , the zonal polynomial can be represented as [58, Eq. (85)],

$$C_{\kappa}(\mathbf{A}) = \chi_{\kappa}(1) \chi_{\kappa}(\mathbf{A}), \quad (96)$$

where

$$\chi_{\kappa}(1) = \frac{k! \prod_{1 \leq i < j \leq n} (\kappa_i - \kappa_j - i + j)}{\prod_{j=1}^n (\kappa_j + n - j)!} \quad (97)$$

and

$$\chi_{\kappa}(\mathbf{A}) = \frac{\det \left(a_i^{\kappa_j + n - j} \right)}{\det \left(a_i^{n - j} \right)} \quad (98)$$

is a Schur polynomial⁵. Schur polynomials form a basis in the space of homogeneous symmetric polynomials in n variables of degree k for all $k \leq n$. In particular, we have [58, Eq. (17)]

$$(\text{Tr} \mathbf{A})^k = \sum_{\kappa} C_{\kappa}(\mathbf{A}). \quad (99)$$

We will need the following identity⁶ [59, Eq. (6.2.3)]

$$\int_{\mathbf{X}} \text{etr}(-\mathbf{XZ}) (\det(\mathbf{X}))^{n-p} {}_r\tilde{F}_s(a_1, \dots, a_r; b_1, \dots, b_s; \mathbf{X}) d\mathbf{X} = {}_{r+1}\tilde{F}_s(a_1, \dots, a_r, n; b_1, \dots, b_s; \mathbf{Z}^{-1}) (\det(\mathbf{Z}))^{-n} \tilde{\Gamma}_p(n), \quad (100)$$

⁵When some eigenvalues of \mathbf{A} are equal, the corresponding Schur polynomials (98) are obtained by using l'Hospital's rule.

⁶ $\text{etr}(\cdot) = e^{\text{Tr}(\cdot)}$ denotes exponential of trace.

where \mathbf{X}, \mathbf{Z} are $p \times p$ Hermitian matrices and $\tilde{\Gamma}_p(n)$ is defined in (37).

We will prove the following lemma.

Lemma 7. *For any $p \times n$ complex matrix \mathbf{S} , we have*

$$\int_{\mathbf{Y} \in \mathcal{V}_{n,p}^{\mathbb{C}}} \text{etr}(\mathbf{S}\mathbf{Y}) d\mu(\mathbf{Y}) = {}_0\tilde{F}_1(n; \mathbf{S}\mathbf{S}^H). \quad (101)$$

where $d\mu(\mathbf{Y})$ is the uniform measure.

Proof: First, note that it is equivalent to showing that

$$(\det \mathbf{S}\mathbf{S}^H)^{n-p} \int_{\mathbf{Y}} \text{etr}(\mathbf{S}\mathbf{Y} + \mathbf{Y}^H \mathbf{S}^H) d\mu(\mathbf{Y}) = (\det \mathbf{S}\mathbf{S}^H)^{n-p} {}_0\tilde{F}_1(n; \mathbf{S}\mathbf{S}^H). \quad (102)$$

We will show that the matrix-variate Laplace transforms of both sides of the above equation are the same.

The Laplace transform of the left-hand-side (LHS) is

$$\begin{aligned} T_{\text{LHS}}(\mathbf{Z}) &= \int_{\mathbf{S}\mathbf{S}^H} \text{etr}(-\mathbf{S}\mathbf{S}^H \mathbf{Z}) (\det \mathbf{S}\mathbf{S}^H)^{n-p} \int_{\mathbf{Y}} \text{etr}(\mathbf{S}\mathbf{Y} + \mathbf{Y}^H \mathbf{S}^H) d\mu(\mathbf{Y}) d(\mathbf{S}\mathbf{S}^H) \\ &= \frac{\tilde{\Gamma}_p(n)}{\pi^{np}} \int_{\mathbf{Y}} \int_{\mathbf{S}} \text{etr}(-\mathbf{S}\mathbf{S}^H \mathbf{Z} + \mathbf{S}\mathbf{Y} + \mathbf{Y}^H \mathbf{S}^H) d\mathbf{S} d\mu(\mathbf{Y}). \end{aligned} \quad (103)$$

The above equality is established by utilizing the decomposition [59, Th. 4.5] $\mathbf{S} = \mathbf{L}\mathbf{U}$ where \mathbf{L} is a $p \times p$ lower triangular matrix with positive diagonal elements and $\mathbf{U}^H \in \mathcal{V}_{n,p}^{\mathbb{C}}$, to lead to the fact that [59, Coroll. 4.5.3]

$$d\mathbf{S} = 2^{-p} (\det \mathbf{S}\mathbf{S}^H)^{n-p} d(\mathbf{S}\mathbf{S}^H) d\nu_{\mathbf{U}}, \quad (104)$$

where here [59, Coroll. 4.5.2] the measure on the Stiefel manifold is normalized so that $\int_{\mathcal{V}_{n,p}^{\mathbb{C}}} d\nu_{\mathbf{U}} = \frac{2^p \pi^{np}}{\tilde{\Gamma}_p(n)}$.

Applying the transform $\mathbf{S} = \mathbf{Z}^{-1/2} \mathbf{T}$ with $d\mathbf{S} = (\det \mathbf{Z})^{-n} d\mathbf{T}$ in (103), we have

$$\begin{aligned} T_{\text{LHS}}(\mathbf{Z}) &= \frac{\tilde{\Gamma}_p(n) (\det \mathbf{Z})^{-n}}{\pi^{np}} \int_{\mathbf{Y}} \int_{\mathbf{T}} \text{etr}(-\mathbf{T}\mathbf{T}^H + \mathbf{Z}^{-1/2} \mathbf{T}\mathbf{Y} + \mathbf{Y}^H \mathbf{T}^H (\mathbf{Z}^{-1/2})^H) d\mathbf{T} d\mu(\mathbf{Y}) \\ &= \frac{\tilde{\Gamma}_p(n) (\det \mathbf{Z})^{-n} \text{etr}(\mathbf{Z}^{-1})}{\pi^{np}} \times \\ &\quad \int_{\mathbf{Y}} \int_{\mathbf{T}} \text{etr}\left(-\left(\mathbf{T} - \mathbf{Y}^H (\mathbf{Z}^{-1/2})^H\right) \left(\mathbf{T} - \mathbf{Y}^H (\mathbf{Z}^{-1/2})^H\right)^H\right) d\mathbf{T} d\mu(\mathbf{Y}) \\ &= \tilde{\Gamma}_p(n) (\det \mathbf{Z})^{-n} \text{etr}(\mathbf{Z}^{-1}), \end{aligned} \quad (105)$$

where the last step is established by the fact that $p(\mathbf{X}) = \frac{1}{\pi^{np}} \text{etr}\left(-(\mathbf{X} - \mathbf{M})(\mathbf{X} - \mathbf{M})^H\right)$ is a matrix-variate Gaussian density function.

The Laplace transform of the right-hand side (RHS) of (102) is

$$\begin{aligned}
T_{\text{RHS}}(\mathbf{Z}) &= \int_{\mathbf{S}\mathbf{S}^H} \text{etr}(-\mathbf{S}\mathbf{S}^H \mathbf{Z}) (\det(\mathbf{S}\mathbf{S}^H))^{n-p} {}_0\tilde{F}_1(n; \mathbf{S}\mathbf{S}^H) d(\mathbf{S}\mathbf{S}^H) \\
&= \tilde{\Gamma}_p(n) (\det(\mathbf{Z}))^{-n} {}_1\tilde{F}_1(n; n; \mathbf{Z}^{-1}) \\
&= \tilde{\Gamma}_p(n) (\det(\mathbf{Z}))^{-n} {}_0\tilde{F}_0(\mathbf{Z}^{-1}) \\
&= \tilde{\Gamma}_p(n) (\det(\mathbf{Z}))^{-n} \text{etr}(\mathbf{Z}^{-1}) = T_{\text{LHS}}(\mathbf{Z}),
\end{aligned} \tag{106}$$

where the second equality is obtained by the identity (100). By the uniqueness of Laplace transforms, we complete the proof of the lemma.

B. Stiefel Manifold

We now prove Lemma 3 in the case of the Stiefel manifold. The expansion of the chordal distance in terms of an inner product in the ambient space gives

$$d_c^2(\mathbf{I}_{n,p}, \mathbf{Y}) = \|\mathbf{I}_{n,p} - \mathbf{Y}\|_F^2 = 2p - 2\Re\text{Tr}(\mathbf{I}_{n,p}^H \mathbf{Y}). \tag{107}$$

Accordingly, define the linear statistic

$$Y = \Re\text{Tr}(\mathbf{I}_{n,p}^H \mathbf{Y}), \tag{108}$$

so that the distance is now expressed as $d_c^2(\mathbf{I}_{n,p}, \mathbf{Y}) = 2p - 2Y$.

This type of linear statistic converges in distribution to a Gaussian random variable as n approaches infinity [33]. To see this, consider the moment generating function of Y which can be represented as a hypergeometric function of matrix argument using Lemma 7 with $\mathbf{S} = \frac{\nu}{2}\mathbf{I}_{n,p}^H$,

$$\begin{aligned}
\mathbb{E}[e^{\nu Y}] &= {}_0\tilde{F}_1\left(n; \frac{\nu^2}{4}\mathbf{I}_{n,p}^H \mathbf{I}_{n,p}\right) \\
&= {}_0\tilde{F}_1\left(n; \frac{\nu^2}{4}\mathbf{I}_p\right).
\end{aligned} \tag{109}$$

Note that it corresponds to the partition function of the von-Mises Fisher distribution [48] with parameter matrix $\nu\mathbf{I}_{n,p}$.

By the definition of the hypergeometric function (94), we can further write

$$\begin{aligned}
\mathbb{E}[e^{\nu Y}] &= \sum_{k=0}^{\infty} \sum_{\kappa} \frac{1}{(n)_{\kappa}} \frac{C_{\kappa}\left(\frac{\nu^2}{4}\mathbf{I}_p\right)}{k!} \\
&= \sum_{k=0}^{\infty} \frac{\left(\frac{\nu^2}{4}\right)^k}{k!} \sum_{\kappa} \frac{C_{\kappa}(\mathbf{I}_p)}{(n)_{\kappa}},
\end{aligned} \tag{110}$$

where the last equality is established by (98). Since the leading order term in $(n - j + 1)_{\kappa_j}$ equals n^{κ_j} , by the definition (95), for large n we have

$$(n)_{\kappa} = \prod_{j=1}^n (n - j + 1)_{\kappa_j} \sim n^{\kappa_1 + \dots + \kappa_n} = n^k. \quad (111)$$

Using (99), the sum in (110) for large n becomes

$$\sum_{\kappa} \frac{C_{\kappa}(\mathbf{I}_p)}{(n)_{\kappa}} \stackrel{n \rightarrow \infty}{=} \frac{1}{n^k} \sum_{\kappa} C_{\kappa}(\mathbf{I}_p) = \frac{1}{n^k} \text{Tr}^k(\mathbf{I}_p) = \frac{p^k}{n^k}, \quad (112)$$

and we arrive at the result,

$$\lim_{n \rightarrow \infty} \mathbb{E} [e^{\nu Y}] = \sum_{k=0}^{\infty} \frac{\left(\frac{\nu^2 p}{4n}\right)^k}{k!} = e^{\frac{\nu^2 p}{4n}}. \quad (113)$$

The distribution corresponds to a Gaussian distribution with zero mean and variance $\frac{p}{2n}$. As a by product the squared chordal distance converges in distribution to a Gaussian random variable

$$d_c^2(\mathbf{I}_{n,p}, \mathbf{Y}) \xrightarrow{d} \mathcal{N}\left(2p, \frac{2p}{n}\right). \quad (114)$$

C. Grassmann Manifold

The case of the Grassmann manifold can be deduced as a by product of the volume computation in [31] by setting $q = p$ (i.e. the dimension of the center of the ball and the elements in the ball have the same dimension). We provide below alternative lines of derivation from the hypergeometric function interpretation consistent with the Stiefel case discussed above.

If \mathbf{Y} is uniformly distributed on the Stiefel manifold, then $[\mathbf{Y}]$ is uniformly distributed on the Grassmann manifold. A point $[\mathbf{Y}]$ on the Grassmann manifold can be uniquely defined by its projection matrix $\Pi_{\mathbf{Y}} = \mathbf{Y}\mathbf{Y}^H$. Looking at uniform measure as a probability measure, the mapping $\mathbf{Y} \rightarrow \Pi_{\mathbf{Y}}$ maps the uniform distribution on $\mathcal{V}_{n,p}^{\mathbb{C}}$ to the uniform distribution on $\mathcal{G}_{n,p}^{\mathbb{C}}$. Namely, if \mathbf{Y} has the same distribution as $\mathbf{U}\mathbf{Y}$ for all $\mathbf{U} \in \mathcal{U}_n$, then $\Pi_{\mathbf{U}\mathbf{Y}}$ has the same distribution as $\mathbf{U}\Pi_{\mathbf{Y}}\mathbf{U}^H$ for all $\mathbf{U} \in \mathcal{U}_n$. Accordingly, consider

$$\begin{aligned} d_c^2([\mathbf{I}_{n,p}], [\mathbf{Y}]) &= \frac{1}{2} \|\mathbf{E} - \Pi_{\mathbf{Y}}\|_F^2 \\ &= p - \text{Tr}(\mathbf{Y}^H \mathbf{E} \mathbf{Y}) \end{aligned} \quad (115)$$

with $\mathbf{E} = \mathbf{I}_{n,p} \mathbf{I}_{n,p}^H$ and such that \mathbf{Y} is uniformly distributed on the Stiefel manifold $\mathcal{V}_{n,p}^{\mathbb{C}}$.

Similarly, we expressed the chordal distance $d_c^2([\mathbf{I}_{n,p}], [\mathbf{Y}]) = p - Z$ as a function of a linear statistic $Z = \text{Tr}(\mathbf{Y}^H \mathbf{E} \mathbf{Y})$. This linear statistic is asymptotically Gaussian for $n, p \rightarrow \infty$ and $n - 2p$ constant as

shown in [31]⁷ through its interpretation as the sum of squared principal cosines distributed according to the Jacobi ensemble [60, Sec. 2.1.2.] and using [61, Th. 2].

The moment-generating function of Z corresponds to the partition function of the Bingham distribution [48] with parameter matrix $\nu \mathbf{E}$, which can be expressed as a confluent hypergeometric function of complex matrix argument. This can be verified by matrix-variate Laplace transforms, similarly as the proof of Lemma 7. It follows that the moments of Z can be computed by identification from the definition of the hypergeometric function (94):

$$\begin{aligned} \mathbb{E}[e^{\nu Z}] &= \sum_{k=0}^{\infty} \frac{\nu^k}{k!} \mathbb{E}[Z^k] \\ &= {}_1\tilde{F}_1(p, n; \nu \mathbf{E}) \\ &= \sum_{k=0}^{\infty} \frac{\nu^k}{k!} \sum_{\kappa} \frac{(p)_{\kappa}}{(n)_{\kappa}} C_{\kappa}(\mathbf{E}). \end{aligned} \quad (116)$$

The mean of Z is given for $k = 1$ for which there is only one partition such that $\chi_{\kappa}(\mathbf{E}) = p$, and $\mathbb{E}[Z] = \frac{p^2}{n}$. For the second moments with $k = 2$, the possible partitions are $\kappa = \{2, 0, \dots, 0\}$ and $\kappa = \{1, 1, 0, \dots, 0\}$. The corresponding Schur polynomials for each partition are $\chi_{\kappa}(\mathbf{E}) = \frac{p}{2}(p+1)$ and $\chi_{\kappa}(\mathbf{E}) = \frac{p}{2}(p-1)$, respectively; while for both partitions one has $\frac{(p)_{\kappa}}{(n)_{\kappa}} = \frac{p(p+1)}{n(n+1)}$ and $\chi_{\kappa}(1) = 1$. One obtains after some manipulations $\mathbb{E}[Z^2] = \frac{p^2(np^2 - 2p + n)}{n(n^2 - 1)}$.

It follows that the squared chordal distance for the Grassmann manifold converges in distribution to a Gaussian random variable

$$d_c^2([\mathbf{I}_{n,p}], [\mathbf{Y}]) \xrightarrow{d} \mathcal{N}\left(\frac{p(n-p)}{n}, \frac{p^2(n-p)^2}{n^2(n^2-1)}\right), \quad (117)$$

where the mean and variance are obtained from the above computations.

APPENDIX E

PROOF OF THE VOLUME COMPARISON IN THEOREM 2

Now with Lemma 3, we are in position to prove Theorem 2. The result follows by identification of the asymptotic forms between the manifold and the embedding sphere.

⁷One has $Z = \sum_{i=1}^p \cos^2 \theta_i$ from the definition of the chordal distance (17). Computing the moment-generating function of this linear statistic one gets $\mathbb{E}[e^{\nu Z}] = e^{p\nu} D_p(i\nu)$ where $D_p(\nu)$ is defined in [31, Eq. (22)].

A. Stiefel Manifold

Identifying the normalized volume of a ball as a probability measure, and without loss of generality, choosing $\mathbf{I}_{n,p}$ as the center, we have

$$\begin{aligned}\mu(B(r)) &= \Pr\{\mathbf{Y} \in \mathcal{V}_{n,p}^{\mathbb{C}} \mid 0 \leq d_c(\mathbf{I}_{n,p}, \mathbf{Y}) \leq r\} \\ &= F_{d_c^2}(r^2) - F_{d_c^2}(0),\end{aligned}\tag{118}$$

where $F_{d_c^2}(z)$ is the cumulative distribution of the random variable $d_c^2(\mathbf{I}_{n,p}, \mathbf{Y})$ with \mathbf{Y} being uniformly distributed on $\mathcal{V}_{n,p}^{\mathbb{C}}$.

As shown in Lemma 3, $d_c^2(\mathbf{I}_{n,p}, \mathbf{Y})$ converges in distribution to a Gaussian random variable with mean $2p$ and variance $\frac{2p}{n}$, and thus

$$F_{d_c^2}(z) \rightarrow \frac{1}{2} \left(1 + \operatorname{erf} \left(\sqrt{np} \left(\frac{z}{2p} - 1 \right) \right) \right).\tag{119}$$

The final asymptotic expression is obtained by replacing the above with $z = r^2$ and $z = 0$ in (118) leading to (49).

Finally, one verifies that the asymptotic volume of a ball in (49) is exactly the asymptotic volume of a cap in the embedding sphere $\mathcal{V}_{n,p}^{\mathbb{C}} \hookrightarrow \mathcal{S}^{2np-1}(\sqrt{p})$ by identification with $D = 2np$ and $R = \sqrt{p}$ in (33).

B. Grassmann Manifold

Again from the results of [31], one may directly obtain (50) and its regime of convergence by setting $q = p$. Alternatively, the volume of a ball of radius r centered around $[\mathbf{I}_{n,p}]$ can be expressed as

$$\begin{aligned}\mu(B(r)) &= \Pr\{[\mathbf{Y}] \in \mathcal{G}_{n,p}^{\mathbb{C}} \mid 0 \leq d_c([\mathbf{I}_{n,p}], [\mathbf{Y}]) \leq r\} \\ &= \Pr\{\mathbf{Y} \in \mathcal{V}_{n,p}^{\mathbb{C}} \mid 0 \leq d_c([\mathbf{I}_{n,p}], [\mathbf{Y}]) \leq r\} \\ &= F_{d_c^2}(r^2) - F_{d_c^2}(0),\end{aligned}\tag{120}$$

where $F_{d_c^2}(z)$ is the cumulative distribution of the random variable $d_c^2([\mathbf{I}_{n,p}], [\mathbf{Y}])$ such that \mathbf{Y} is uniformly distributed on the Stiefel manifold $\mathcal{V}_{n,p}^{\mathbb{C}}$.

As shown in Lemma 3, the squared chordal distance for the Grassmann manifold converges in distribution to a Gaussian random variable with mean $\frac{p(n-p)}{n}$ and variance $\frac{p^2(n-p)^2}{n^2(n^2-1)}$ so that its cumulative distribution is given by

$$F_{d_c^2}(z) \rightarrow \frac{1}{2} \left(1 + \operatorname{erf} \left(\sqrt{\frac{n^2(n^2-1)}{2p^2(n-p)^2}} \left(z - \frac{p(n-p)}{p} \right) \right) \right).\tag{121}$$

The final asymptotic expression is obtained by replacing the above with $z = r^2$ and $z = 0$ in (120) leading to (50) after some simplifications.

Finally, one verifies also here that the asymptotic volume of a ball in (50) equals the asymptotic volume of a cap in the embedding sphere $\mathcal{G}_{n,p}^C \hookrightarrow \mathcal{S}^{n^2-2} \left(\sqrt{\frac{p(n-p)}{2n}} \right)$ by identification with $D = n^2 - 1$ and $R = \sqrt{\frac{p(n-p)}{2n}}$ in (33).

APPENDIX F

PROOF OF KISSING RADIUS BOUNDS IN PROPOSITION 1

Consider a code $\mathcal{C} = \{\mathbf{C}_1, \dots, \mathbf{C}_N\}$ with pairwise distances among the codewords $\{\delta_{i,j}\}_{i \neq j}$ such that $\delta = \min\{\delta_{i,j}\}$. Between each codeword there is a different mid-distance $\{\varrho_{i,j}\}_{i \neq j}$ and the kissing radius $\varrho = \min \varrho_{i,j}$. The detailed derivations below provide a lower and upper bound on a mid-distance $\underline{\varrho}(\delta_{i,j}) \leq \varrho_{i,j} \leq \bar{\varrho}(\delta_{i,j})$ as function of the distance $\delta_{i,j}$. It can be verified that the obtained bounds $\underline{\varrho}$ and $\bar{\varrho}$ are increasing functions. It then follows that $\min\{\underline{\varrho}(\delta_{i,j})\} = \underline{\varrho}(\min\{\delta_{i,j}\})$ and $\min\{\bar{\varrho}(\delta_{i,j})\} = \bar{\varrho}(\min\{\delta_{i,j}\})$, and one has $\underline{\varrho}(\delta) \leq \varrho \leq \bar{\varrho}(\delta)$.

A. Grassmann Manifold

The principal angles $\boldsymbol{\theta} = (\theta_1, \dots, \theta_p)$ between two codewords $\mathbf{C}_i, \mathbf{C}_j$ separated by δ satisfies $\sum_{i=1}^p \sin^2(\theta_i) = \delta^2$. Without loss of generality, the code may be rotated so that the Stiefel representatives of these codewords are of the form $\mathbf{C}_i = \mathbf{I}_{n,p}$ and $\mathbf{C}_j = [(\text{diag}(\cos \boldsymbol{\theta}) \text{diag}(\sin \boldsymbol{\theta}))^T]$ [15].

The chordal distance is measured along the geodesic. The principal angles between the midpoint $\mathbf{C}_{i,j}$ (on the geodesic joining \mathbf{C}_i and \mathbf{C}_j) and a codeword \mathbf{C}_i or \mathbf{C}_j are $(\frac{\theta_1}{2}, \dots, \frac{\theta_p}{2})$ [16]. It follows that the squared chordal distance between the midpoint on the geodesic and an extremity of the geodesic is

$$\varrho^2 = \left\| \sin \frac{\boldsymbol{\theta}}{2} \right\|_2^2 = \sum_{i=1}^p \sin^2 \frac{\theta_i}{2}. \quad (122)$$

Finding lower and upper bounds reduces to solving the following optimization problems:

$$\begin{aligned} & \underset{\boldsymbol{\theta} \in [0, \frac{\pi}{2}]^p}{\text{minimize/maximize}} && \left\| \sin \frac{\boldsymbol{\theta}}{2} \right\|_2^2 \\ & \text{subject to} && \left\| \sin \boldsymbol{\theta} \right\|_2^2 = \delta^2. \end{aligned} \quad (123)$$

First, to find the minimum, consider the corresponding Lagrange function

$$\Lambda(\theta_1, \dots, \theta_p, \lambda) = \left\| \sin \frac{\boldsymbol{\theta}}{2} \right\|_2^2 + \lambda \left(\left\| \sin \boldsymbol{\theta} \right\|_2^2 - \delta^2 \right). \quad (124)$$

Solving:

$$\frac{\partial \Lambda}{\partial \theta_i} = \sin \theta_i (1/2 + 2\lambda \cos \theta_i) = 0 \quad \text{for } i = 1 \dots p \quad (125)$$

$$\frac{\partial \Lambda}{\partial \lambda} = \sum_{i=1}^p \sin^2 \theta_i - \delta^2 = 0 \quad (126)$$

yields a set of stationary points where at least x angles are nonzero such that $x \geq \lceil \delta^2 \rceil$ and equal to $\theta^* = \arcsin \frac{\delta}{\sqrt{x}}$. It is then easy to verify that the objective function $f(x) = \sum_{i=1}^p \sin^2 \frac{\theta_i}{2} = x/2(1 - \sqrt{1 - \delta^2/x})$ is a strictly decreasing function on $[\lceil \delta^2 \rceil, p]$ and thus is minimized for $x = p$. The result follows.

Maximization in (123) is obtained when a minimum number of angles is maximized, i.e., with $(\theta_1^*, \dots, \theta_p^*) \in [0, \frac{\pi}{2}]^p$ such that $\theta_1^* = \dots = \theta_{\lceil \delta^2 \rceil}^* = \frac{\pi}{2}$, $\theta_{\lceil \delta^2 \rceil}^* = \arcsin(\sqrt{\delta^2 - \lceil \delta^2 \rceil})$ and $\theta_{\lceil \delta^2 \rceil + 1}^* = \dots = \theta_p^* = 0$.

This can be verify by contradiction: Defining $s_i = \sin^2 \theta_i$ and $t(s_i) = (1 - \sqrt{1 - s_i})/2$, consider the equivalent problem of maximizing $\sum t(s_i)$ such that $\sum s_i = \delta^2$ and without loss of generality $1 \geq s_1 \geq s_2 \dots \geq s_p \geq 0$. By contradiction, assume that $\sum t(s_i)$ is maximum at \mathbf{a} with $a_i > 0 \forall i$. It is possible to find a \mathbf{b} with $b_i \geq a_i$ for $1 \leq i \leq p-1$ and $b_p = 0$. Since $t'(\cdot)$ is strictly increasing, it follows from the mean value theorem that there exist $c \in (a_{p-1}, b_{p-1})$ and $d \in (0, a_p)$ such that

$$\sum t(b_i) - t(a_i) \geq t'(c) \sum_{i=1}^{p-1} (b_i - a_i) + t'(d)(a_p - b_p) \quad (127)$$

$$= (t'(d) + t'(c))a_p > 0, \quad (128)$$

where the last equality is due to the constraint $\sum b_i = \sum a_i = \delta^2$, which is in contradiction with the fact that $\sum t(a_i)$ is a maximum. Repeating the procedure from s_p to $s_{\lceil \delta^2 \rceil}$ leads to the results. Lastly, the maximum is

$$\begin{aligned} \sum_{i=1}^p \sin^2 \frac{\theta_i^*}{2} &= \frac{\lfloor \delta^2 \rfloor}{2} + \frac{1 - \sqrt{1 - (\delta^2 - \lfloor \delta^2 \rfloor)}}{2} \\ &= \frac{1}{2} \left(\lceil \delta^2 \rceil - \sqrt{\lceil \delta^2 \rceil - \delta^2} \right). \end{aligned} \quad (129)$$

B. Unitary Group

A simple adaptation of the proof for the unitary group can be done, see also [17] where similar optimization problems are considered. Consider a unitary code \mathcal{C} with minimum distance δ . The angles $(\theta_1, \dots, \theta_n)$ between two codewords $\mathbf{C}_i, \mathbf{C}_j$ separated by δ now satisfies $\sum_{i=1}^n \sin^2(\frac{\theta_i}{2}) = \frac{\delta^2}{4}$. Again, the chordal distance is measured along the geodesic and the principal angles between the midpoint and

a codeword are $(\frac{\theta_1}{2}, \dots, \frac{\theta_p}{2})$. It follows that the squared chordal distance between the midpoint on the geodesic and an extremity of the geodesic is

$$\varrho^2 = 4 \sum_{i=1}^n \sin^2 \frac{\theta_i}{4}. \quad (130)$$

Finding lower and upper bounds reduces to solving the following optimization problems:

$$\begin{aligned} & \underset{\boldsymbol{\theta} \in [-\pi, \pi]^n}{\text{minimize/maximize}} && 4 \|\sin \frac{\boldsymbol{\theta}}{4}\|_2^2 \\ & \text{subject to} && \|\sin \frac{\boldsymbol{\theta}}{2}\|_2^2 = \frac{\delta^2}{4}. \end{aligned} \quad (131)$$

By using the change of variables $\phi = (\boldsymbol{\theta} + \pi)/2$, $\gamma = \frac{\delta}{2}$ and $\rho = \frac{\rho}{2}$, we recover the optimization problem (123). The result follows.

C. Stiefel Manifold

For a generic Stiefel manifold, the notion of principal angles does not exist. The obtained lower bound for the unitary group is actually matching the kissing radius bound from the spherical embedding. This result thus directly extends to all Stiefel manifolds. However, we were not able to generalize the upper bound. We provide some discussion below.

Without loss of generality, we can assume that the first point is $\mathbf{I}_{n,p}$ and the second point is \mathbf{Y} . If \mathbf{Y} is block unitary as $\mathbf{Y} = [\mathbf{U} \ \mathbf{0}]^T$, where $\mathbf{U} \in \mathcal{U}_p$ then the geodesic between this two points stays in \mathcal{U}_p embedded in $\mathcal{V}_{n,p}^{\mathbb{C}}$, and the upper bound from the unitary group would apply.

For a generic \mathbf{Y} , the distance only depends on the diagonal element of $\mathbf{Y} = \{Y_{ij}\}$:

$$\begin{aligned} d_c^2(\mathbf{I}_{n,p}, \mathbf{Y}) &= 2(p - \Re(\text{Tr}(\mathbf{I}_{n,p}^H \mathbf{Y}))) = 2 \left(p - \sum_{i=1}^p \Re(Y_{ii}) \right) \\ &= 2 \left(p - \sum_{i=1}^p \cos \theta_i \right) = 4 \sum_{i=1}^p \sin^2 \frac{\theta_i}{2} \\ &= p \sin^2 \theta, \end{aligned} \quad (132)$$

where without of loss of generality, we can write $\cos \theta_i = \Re(Y_{ii})$ and $\cos \theta = \frac{1}{p} \sum_{i=1}^p \cos \theta_i$. The angles $\{\theta_i\}$ then correspond the canonical embedding of the Stiefel manifold in $(\mathcal{S}^{2n-1})^p$, the angle θ to the embedding in $\mathcal{S}^{2np-1}(\sqrt{p})$.

The geodesic is not along these angles, and the midpoint, say $\mathbf{M}_{\mathbf{Y}}$, on the geodesic is not at $\{\frac{\theta_i}{2}\}$ nor at $\frac{\theta}{2}$. However since we have an isometry for these embeddings,

$$d_c^2(\mathbf{I}_{n,p}, \mathbf{M}_{\mathbf{Y}}) \geq 2 \left(p - \sum_{i=1}^p \cos \frac{\theta_i}{2} \right) = 4 \sum_{i=1}^p \sin^2 \frac{\theta_i}{4} \quad (133)$$

$$\geq p \sin^2 \frac{\theta}{2}. \quad (134)$$

From this, by maximizing the right hand-side of the first inequality, we can deduce that the maximum is greater or equal to the upper bound of the unitary group, i.e.

$$\max_{\mathbf{Y}} d^2(\mathbf{I}_{n,p}, \mathbf{M}_{\mathbf{Y}}) \geq \bar{\varrho}. \quad (135)$$

A generalization would imply that $\max_{\mathbf{Y}} d^2(\mathbf{I}_{n,p}, \mathbf{M}_{\mathbf{Y}}) = \bar{\varrho}$. We finally note that the midpoint $\mathbf{M}_{\mathbf{Y}}$ can be computed by an orthogonal projection of the center of mass $\frac{1}{2}(\mathbf{I}_{n,p} + \mathbf{Y})$ to the Stiefel manifold, which is given by the polar decomposition⁸.

D. Proof of Corollary 2

For the Grassmann manifold with $R^2 = \frac{p(n-p)}{2n}$, it can be easily verified that $p \leq 4R^2$ with equality if and only if $p = n/2$. Then, since $x/2(1 - \sqrt{1 - \delta^2/x})$ is a strictly decreasing function, it follows that $\varrho_s \leq \underline{\varrho}$ with equality if and only if $p = n/2$.

REFERENCES

- [1] R. A. Rankin, "The closest packing of spherical caps in n dimensions," *Proc. Glasgow Math. Assoc.*, vol. 2, pp. 139–144, 1955.
- [2] C. A. Rogers, "The packing of equal spheres," *Proc. London Math. Soc.*, vol. 8, p. 609620, 1958.
- [3] L. Tóth, "Distribution of points in the elliptic plane," *Acta Math. Hungar.*, vol. 16, no. 3-4, pp. 437–440, 1965.
- [4] J. H. Conway and N. J. A. Sloane, *Sphere Packings, Lattices and Groups*. Springer-Verlag, New York, 2nd edition, 1993.
- [5] C. E. Shannon, "A mathematical theory of communication," *Bell Syst. Tech. J.*, vol. 27, no. 4, pp. 623–656, Oct. 1948.
- [6] L. Zheng and D. Tse, "Communication on the Grassmann manifold: a geometric approach to the noncoherent multiple-antenna channel," *IEEE Trans. Inf. Theory*, vol. 48, no. 2, pp. 359–383, Feb. 2002.
- [7] D. Agrawal, T. Richardson, and R. Urbanke, "Multiple-antenna signal constellations for fading channels," *IEEE Trans. Inf. Theory*, vol. 47, no. 6, pp. 2618–2626, Sept. 2001.
- [8] D. J. Love, R. W. Heath Jr., and T. Strohmer, "Grassmannian beamforming for multiple-input multiple-output wireless systems," *IEEE Trans. Inf. Theory*, vol. 49, no. 10, pp. 2735–2747, Oct. 2003.
- [9] D. Love and R. Heath, "Limited feedback unitary precoding for spatial multiplexing systems," *IEEE Trans. Inf. Theory*, vol. 51, no. 8, pp. 2967–2976, Aug. 2005.
- [10] K. K. Mukkavilli, A. Sabharwal, E. Erkip, and B. Aazhang, "On beamforming with finite rate feedback in multiple-antenna systems," *IEEE Trans. Inf. Theory*, vol. 49, no. 10, pp. 2562–2579, Oct. 2003.
- [11] R.-A. Pitaval and O. Tirkkonen, "Joint Grassmann-Stiefel quantization for MIMO product codebook," *IEEE Trans. Wireless Commun.*, vol. 13, no. 1, pp. 210–222, Feb. 2014.
- [12] R. Heath, T. Strohmer, and A. Paulraj, "On quasi-orthogonal signatures for CDMA systems," *IEEE Trans. Inf. Theory*, vol. 52, no. 3, pp. 1217–1226, Mar. 2006.

⁸Except if $\mathbf{I}_{n,p}$ and \mathbf{Y} are antipodal then their center of mass is $\mathbf{0}$ and it does not have a unique projection.

- [13] A. Ashikhmin and A. Calderbank, “Grassmannian packings from operator Reed-Müller codes,” *IEEE Trans. Inf. Theory*, vol. 56, no. 11, pp. 5689–5714, Nov. 2010.
- [14] R. Calderbank, A. Thompson, and Y. Xie, “On block coherence of frames,” *Appl. Comput. Harmon. Anal.*, vol. 38, no. 1, pp. 50–71, 2015.
- [15] J. H. Conway, R. H. Hardin, and N. J. A. Sloane, “Packing lines, planes, etc.: Packings in Grassmannian space,” *Exper. Math.*, vol. 5, pp. 139–159, 1996.
- [16] A. Edelman, T. Arias, and S. T. Smith, “The geometry of algorithms with orthogonality constraints,” *SIAM J. Matrix Anal. Appl.*, vol. 20, no. 2, pp. 303–353, 1998.
- [17] G. Han and J. Rosenthal, “Unitary space-time constellation analysis: An upper bound for the diversity,” *IEEE Trans. Inf. Theory*, vol. 52, no. 10, pp. 4713–4721, Oct. 2006.
- [18] O. Henkel, “Sphere packing bounds in the Grassmann and Stiefel manifolds,” *IEEE Trans. Inf. Theory*, vol. 51, pp. 3445–3456, Oct. 2005.
- [19] A. Barg and D. Nogin, “Bounds on packings of spheres in the Grassmann manifold,” *IEEE Trans. Inf. Theory*, vol. 48, no. 9, pp. 2450–2454, Sept. 2002.
- [20] —, “A bound on Grassmannian codes,” in *Proc. IEEE Int. Symp. Inf. Theory*, July 2006, pp. 997–1000.
- [21] C. Bachoc, “Linear programming bounds for codes in Grassmannian spaces,” *IEEE Trans. Inf. Theory*, vol. 52, no. 5, pp. 2111–2125, May 2006.
- [22] C. Bachoc, Y. Ben-Haim, and S. Litsyn, “Bounds for codes in products of spaces, Grassmann, and Stiefel manifolds,” *IEEE Trans. Inf. Theory*, vol. 54, no. 3, pp. 1024–1035, Mar. 2008.
- [23] J. Creignou and H. Diet, “Linear programming bounds for unitary space time codes,” in *Proc. IEEE Int. Symp. Inf. Theory*, July 2008, pp. 1073–1077.
- [24] W. Dai, Y. Liu, and B. Rider, “Quantization bounds on Grassmann manifolds and applications to MIMO communications,” *IEEE Trans. Inf. Theory*, vol. 54, no. 3, pp. 1108–1123, Mar. 2008.
- [25] R. Krishnamachari and M. Varanasi, “Volume of geodesic balls in the real Stiefel manifold,” in *Proc. 42nd Annu. Conf. Inf. Sci. Syst.*, Mar. 2008, pp. 402–406.
- [26] —, “Volume of geodesic balls in the complex Stiefel manifold,” in *Proc. of Allerton Conf. on Comm. Cont. and Comp.*, Sept. 2008, pp. 902–909.
- [27] W. Dai, B. Rider, and Y. Liu, “Volume growth and general rate quantization on Grassmann manifolds,” in *Proc. IEEE Global Telecom. Conf.*, Nov. 2007, pp. 1441–1445.
- [28] J. Nash, “C1 isometric imbeddings,” *Ann. of Math. (2)*, vol. 60, no. 3, pp. pp. 383–396, 1954.
- [29] L. Wei, R.-A. Pitaval, J. Corander, and O. Tirkkonen, “On the volume of a metric ball in unitary group,” in *IEEE Int. Symp. Inf. Theory*, June 2015, pp. 191–195.
- [30] —, “From random matrix theory to coding theory: Volume of a metric ball in unitary group,” *arXiv preprint*, 2015, arXiv:1508.01358.
- [31] R.-A. Pitaval, L. Wei, O. Tirkkonen, and J. Corander, “Volume of metric balls in high-dimensional complex Grassmann manifolds,” *IEEE Trans. Inf. Theory*, vol. 62, no. 9, pp. 5105–5116, Sep. 2016.
- [32] E. Borel, “Sur les principes de la theorie cinétique des gaz,” *Ann. Sci. l’École Norm. Supér.*, vol. 23, pp. 9–32, 1906.
- [33] D. S. P. Richards, “High-dimensional random matrices from the classical matrix groups, and generalized hypergeometric functions of matrix argument,” *Symmetry*, vol. 3, pp. 600–610, 2011.

- [34] J. Breuer and M. Duits, “Central limit theorems for biorthogonal ensembles and asymptotics of recurrence coefficients,” *arXiv preprint arXiv:1309.6224*, *J. Amer. Math. Soc.*, to appear.
- [35] P. Sole, “Packing radius, covering radius, and dual distance,” *IEEE Trans. on Inf. Theory*, vol. 41, no. 1, pp. 268–272, Jan. 1995.
- [36] A. Schenk, R. Fischer, and L. Lampe, “A stopping radius for the sphere decoder and its application to MSDD of DPSK,” *IEEE Comm. Letters*, vol. 13, no. 7, pp. 465–467, July 2009.
- [37] A. Schenk and R. Fischer, “A stopping radius for the sphere decoder: Complexity reduction in multiple-symbol differential detection,” in *Proc. Int. ITG Conf. Source and Channel Coding*, Jan. 2010, pp. 1–6.
- [38] H.-C. Wang, “Two-point homogeneous spaces,” *Ann. Math.*, vol. 55, no. 1, pp. 177–191, Jan. 1952.
- [39] I. S. Dhillon, R. W. Heath Jr, T. Strohmer, and J. A. Tropp, “Constructing packings in Grassmannian manifolds via alternating projection,” *Experimental Mathematics*, vol. 17, no. 1, pp. 9–35, 2008.
- [40] R.-A. Pitaval, H.-L. Maattanen, K. Schober, O. Tirkkonen, and R. Wichman, “Beamforming codebooks for two transmit antenna systems based on optimum Grassmannian packings,” *IEEE Trans. Inf. Theory*, vol. 57, no. 10, pp. 6591–6602, Oct. 2011.
- [41] J. Creignou, “Constructions of Grassmannian simplices,” *eprint arXiv:cs/0703036*, Mar. 2007.
- [42] L. K. Hua, *Harmonic Analysis of Functions of Several Variables in the Classical Domains*. American Mathematical Society: Providence, Chinese original 1958, Russian translation, Moskva 1959.
- [43] K. Zyczkowski and H.-J. Sommers, “Hilbert-Schmidt volume of the set of mixed quantum states,” *J. Phys. A: Math. Gen.*, vol. 36, no. 39, pp. 10 115–10 130, 2003.
- [44] I. Kim, S. Park, D. Love, and S. Kim, “Improved multiuser MIMO unitary precoding using partial channel state information and insights from the Riemannian manifold,” *IEEE Trans. Wireless Commun.*, vol. 8, no. 8, pp. 4014–4023, Aug. 2009.
- [45] A. Gray, “The volume of a small geodesic ball of a Riemannian manifold,” *Michigan Math. J.*, vol. 20, no. 4, pp. 329–344, 1974.
- [46] M. Belkin and P. Niyogi, “Towards a theoretical foundation for laplacian-based manifold methods,” *J. Comput. Syst. Sci.*, vol. 74, no. 8, pp. 1289–1308, 2008.
- [47] M. Belkin, “Problems of learning on manifolds,” Ph.D. dissertation, University of Chicago, 2003.
- [48] Y. Chikuse, *Statistics on special manifolds*. Lecture Notes in Statistics 174, Springer, New York, 2003.
- [49] R. Bott and L. W. Tu, *Differential forms in algebraic topology*. Springer – Verlag, 1982.
- [50] B. W. Clare and D. L. Kepert, “The closest packing of equal circles on a sphere,” *Proc. Roy. Soc. London Ser. A*, vol. 405, no. 1829, pp. 329–344, 1986.
- [51] P. Xia, S. Zhou, and G. Giannakis, “Achieving the Welch bound with difference sets,” *IEEE Trans. Inf. Theory*, vol. 51, no. 5, pp. 1900–1907, May 2005.
- [52] R.-A. Pitaval, O. Tirkkonen, and S. Blostein, “Low complexity MIMO precoding codebooks from orthoplex packings,” in *Proc. IEEE Int. Conf. Commun.*, June 2011, pp. 1–5.
- [53] S. Li, “Concise formulas for the area and volume of a hyperspherical cap,” *Asian J. Math. Stat.*, vol. 4, no. 1, pp. 66–70, 2011.
- [54] “NIST Digital Library of Mathematical Functions,” <http://dlmf.nist.gov/>, Release 1.0.10 of 2015-08-07, online companion to [55]. [Online]. Available: <http://dlmf.nist.gov/>
- [55] F. W. J. Olver, D. W. Lozier, R. F. Boisvert, and C. W. Clark, Eds., *NIST Handbook of Mathematical Functions*. New York, NY: Cambridge University Press, 2010, print companion to [54].

- [56] L. Pastur and M. Shcherbina, *Eigenvalue Distribution of Large Random Matrices*. American Mathematical Society, 2011.
- [57] A. Edelman, “Eigenvalues and condition numbers of random matrices,” Ph.D. dissertation, Massachusetts Institute of Technology, 1989.
- [58] A. T. James, “Distributions of matrix variates and latent roots derived from normal samples,” *Ann. Math. Statist.*, vol. 35, no. 2, pp. 475–501, May 1964.
- [59] A. M. Mathai, *Jacobians of Matrix Transformations and Functions of Matrix Arguments*. Singapore: World Scientific, 1997.
- [60] I. M. Johnstone, “Multivariate analysis and jacobi ensembles: Largest eigenvalue, Tracy–Widom limits and rates of convergence,” *Ann. Stat.*, vol. 36, no. 6, pp. 2638–2716, 2008.
- [61] K. Johansson, “On random matrices from the compact classical groups,” *Ann. Math.*, vol. 145, no. 3, pp. 519–545, May 1997.